remote sensing

MDPI

Review

Remote Sensing of Environmental Drivers Influencing the Movement Ecology of Sympatric Wild and Domestic Ungulates in Semi-Arid Savannas, a Review

Florent Rumiano [1,2,*], Elodie Wielgus [3,4,5,6,7], Eve Miguel [8,9], Simon Chamaillé-Jammes [6,7,10], Hugo Valls-Fox [6,7,11,12], Daniel Cornélis [13,14], Michel De Garine-Wichatitsky [4,5,15], Hervé Fritz [7,16,17], Alexandre Caron [4,5,18] and Annelise Tran [1,2,4,5]

1 CIRAD, UMR TETIS, F-97490 Sainte-Clotilde, Réunion, France; annelise.tran@cirad.fr
2 TETIS, Univ Montpellier, AgroParisTech, CIRAD, CNRS, INRAE, 34090 Montpellier, France
3 Division of Biology and Conservation Ecology, Manchester Metropolitan University, Manchester M1 5GD, UK; elodie.wielgus@stu.mmu.ac.uk
4 CIRAD, UMR ASTRE, F-34398 Montpellier, France; michel.de_garine-wichatitsky@cirad.fr (M.D.G.-W.); alexandre.caron@cirad.fr (A.C.)
5 ASTRE, Univ Montpellier, CIRAD, INRAE, 34090 Montpellier, France
6 CEFE, Univ. Montpellier, CNRS, EPHE, IRD, Univ. Paul Valéry Montpellier 3, 34090 Montpellier, France; simon.chamaille@cefe.cnrs.fr (S.C.-J.); hugo.valls-fox@cirad.fr (H.V.-F.)
7 LTSER France, Zone Atelier CNRS "Hwange", Hwange National Park, Bag 62 Dete, Zimbabwe; herve.fritz@cnrs.fr
8 MIVEGEC, Univ. Montpellier, IRD, CNRS, 34090 Montpellier, France; eve.miguel@ird.fr
9 CREES Centre for Research on the Ecology and Evolution of DiseaSe–Montpellier, 34090 Montpellier, France
10 Mammal Research Institute, Department of Zoology & Entomology, University of Pretoria, 0083 Pretoria, South Africa
11 CIRAD, UMR SELMET, PPZS, 6189 Dakar, Senegal
12 SELMET, Univ. Montpellier, CIRAD, INRAE, Institut Agro, 34090 Montpellier, France
13 CIRAD, Forêts et Sociétés, F-34398 Montpellier, France; daniel.cornelis@cirad.fr
14 Forêts et Sociétés, Univ. Montpellier, CIRAD, 34090 Montpellier, France
15 Faculty of Veterinary Medicine, Kasetsart University, Bangkok 10900, Thailand
16 UCBL, UMR CNRS 5558, University of Lyon, 69007 Lyon, France
17 World Wildlife Fund, Washington, DC 20037-1193, USA
18 Faculdade de Veterinaria, Universidade Eduardo Mondlane, 257 Maputo, Mozambique
* Correspondence: florent.rumiano@cirad.fr; Tel.: +33-638-2526-72

Received: 31 August 2020; Accepted: 28 September 2020; Published: 2 October 2020

Abstract: Interfaces between protected areas and their peripheries in southern Africa are subject to interactions between wildlife and livestock that vary in frequency and intensity. In these areas, the juxtaposition between production and conservation land uses in a context of increasing anthropisation can create issues associated with human-wildlife coexistence and raises concerns for biodiversity conservation, local development and livelihoods. This literature review aimed at addressing the need to consolidate and gather in one article current knowledge on potential uses of satellite remote sensing (SRS) products by movement ecologists to investigate the sympatry of wildlife/domestic ungulates in savanna interface environments. A keyword querying process of peer reviewed scientific paper, thesis and books has been implemented to identify references that (1) characterize the main environmental drivers impacting buffalo (*Syncerus caffer caffer*) and cattle (*Bos taurus & Bos indicus*) movements in southern Africa environments, (2) describe the SRS contribution to discriminate and characterize these drivers. In total, 327 references have been selected and analyzed. Surface water, precipitation, landcover and fire emerged as key drivers impacting the buffalo and cattle movements. These environmental drivers can be efficiently characterized by SRS, mainly through open-access

SRS products and standard image processing methods. Applying SRS to better understand buffalo and cattle movements in semi-arid environments provides an operational framework that could be replicated in other type of interface where different wild and domestic species interact. There is, however, a need for animal movement ecologists to reinforce their knowledge of remote sensing and/or to increase pluridisciplinary collaborations.

Keywords: African savanna; animal movements; earth observation imagery; remote sensing; sympatric wild and domestic ungulates; wildlife-livestock interface

1. Introduction

In Africa, human populations living at the edge of protected areas have significantly increased in recent years [1,2]. This burst in human population is a challenge for biodiversity conservation in protected areas (PA) and livestock production in adjacent communal lands (CL) where these land uses coexist [3]. At the PA-CL interfaces, interactions between wildlife, people and their livestock frequently occur [4,5] even when park or veterinary fences, largely detrimental to wildlife movements, exist [6–8]. This growing number of interactions potentially increases human/wildlife coexistence related issues [3] such as competition for resources inside/outside protected areas [9], predation of livestock by wild carnivores [10], crop destruction by wildlife [11], and risk of pathogen transmission between wild and domesticated species [12–14]. These complications associated with human/wildlife coexistence raise challenges for biodiversity conservation and local development. They impact local communities' livelihoods and well-being [15–18], and threaten the sustainable coexistence between stakeholders involved in the management of these land-uses. In this context, identifying and characterizing environmental drivers that condition animal movements in space and time is essential to assess the potential opportunities and threats associated with wild/domestic interactions in PA-CL interfaces.

The potential for SRS applications, regarding environment monitoring in general and animal conservation in particular, has been largely stressed [19,20]. Indeed, SRS techniques provide an increasing number of sensors [21–26] that may characterize the environmental drivers impacting animal movements at different space and time scales. Moreover, SRS offers continuous temporal follow-up data in areas where in-situ data are nonexistent and/or difficult to collect [27], as it is the case in the savanna landscapes in southern African PA-CL interfaces [28]. In these heterogeneous open environments with high variability in soil composition, topography, and subject to dynamic processes such as rainfall, fire, climate change, herbivory and human impacts [29–31], SRS could provide viable tools to predict biophysical measurements of cover, density, and biomass of savanna vegetation [32,33]. However SRS also faces difficulties in retrieving vegetation spectral response due to soil background, vegetation shadow, standing dead vegetation occurring in these arid and semi-arid areas [34,35]. Despite these limitations, combining SRS with recent advances in telemetry technology is key to assess wildlife/domestic animal interactions in savanna landscapes, especially at PA-CL interfaces [36–38].

The African buffalo (*Syncerus caffer caffer*) and cattle (*Bos taurus & Bos indicus*) are keystone species for conservation and production systems in southern African PA-CL interfaces. The understanding of their functional ecology constitutes an applied example on how SRS can be efficiently used to design a framework of animal movement analyses. The African buffalo is one of the "Big Five" [39] and contributes to consumptive and non-consumptive tourism [40,41], provides a source of proteins and income for local communities [42] and is an important member of the ungulate guild who shapes habitat heterogeneity in and outside protected areas where the human presence is low [43–46]. Cattle, in subsistence farming communities, provide draught power, source of protein, cash incomes, safety net and social status [47–49]. Buffalo and cattle are both grazer ungulates, close phylogenetically, sharing common resources (i.e., forage and water) [50], and are thus likely to overlap in range and compete for resources, particularly in environments where resources are spatially segregated

(e.g., savannas) [51,52]. Both species rely on their behavior and the management of the land use by humans to cope with constrained access to natural resources (e.g., access to artificial water, forage intake by the herder) [53,54]. Their shared use of space increases the likelihood of direct (i.e., the use of the same space at the same time) and indirect (i.e., the use of the same space at different times) contacts, which in turn promotes the risk of pathogen transmission [12,55–58], a threat to farmers and biodiversity conservation [4,13]. Given this complex ecological context, characterizing buffalo and cattle habitats to understand their movements in space and time in conjunction with currently available SRS applications and methodologies is necessary.

In this review article, we aim at (1) reviewing the main environmental drivers impacting buffalo and cattle movements in southern Africa interface environments, (2) describing the SRS contribution to discriminate and characterize these drivers in southern Africa interfaces. The underlying objective is to facilitate the uses of SRS by movement ecologists in order to improve wildlife/domestic animals management and conservation in different types of savanna interfaces across the globe. It is adding and completing previous works that focused on the link between SRS, environmental challenges and animal movement but in a wider ecological context [20,59].

2. Review Article Methodology

A literature review of peer-reviewed articles, thesis and books in English (such as defined in Grant and Booth (2009) [60]) has been conducted on the following topics: (i) behavioral and movement ecology of buffalo and cattle in southern Africa; (ii) existing remote sensing tools allowing the discrimination in time and space of determined environmental drivers. The Web of Science database was used to retrieve relevant references via a two steps keyword querying process without time constraint. At each step, a systematic screening based on the title and the abstract was first conducted to select the articles, books or thesis for full-text reading. Selected references bibliographies have also been read to extract additional relevant articles, book or thesis.

The first step was to discriminate the environmental drivers impacting buffalo and cattle movements in space and time. The different keywords combined in no particularly order in the first step were “buffalo”; “syncerus caffer”; “cattle”; “bos taurus”; “bos indicus”; “ungulates”; “southern africa”; “movement”. The search resulted in 787 references. After abstract screening and the removal of replicates, 87 peer-reviewed articles, thesis and books from 1975 to 2020 were included in the review (Figure 1). Among them, 29 (33.3%) articles concerned buffalo only, 15 (17.2%) cattle only, and 43 (49.5%) both species. Landcover & Vegetation, surface water, precipitation and savanna fire emerged as main environmental drivers impacting focal species (buffalo & cattle) (Figure 1).

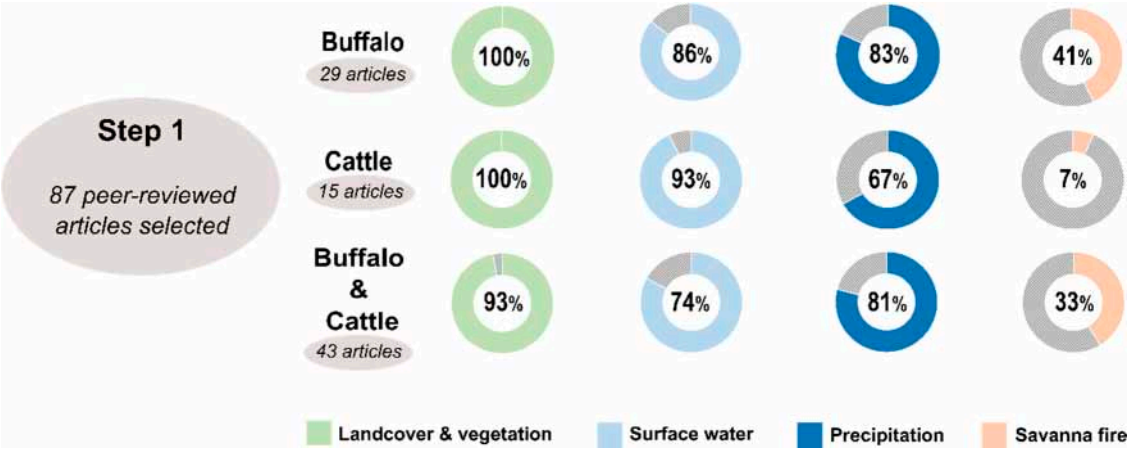

Figure 1. Environmental driver statistics of the step 1 bibliography. The percentage of articles identifying the environmental drivers of animal movements among all the peer-reviewed selected articles is presented according to the species considered (buffalo only, cattle only, buffalo & cattle).

The second step was to define the existing methodologies in remote sensing to characterize the different environmental drivers previously determined. The different keywords combined in no particularly order in the second step were all the environmental drivers determined in the first step: "surface water"; "precipitation"; "rainfall"; "vegetation"; "fire" with the addition of the following keywords: "remote sensing"; "Earth observation imagery"; "landcover"; "land-use"; "spectral index"; "radar"; "optical"; "savanna". The search resulted in 1140 references and, after abstract sreening and the removal of duplicates, 240 articles from 1974 to 2020 were included in the review.

In total, 327 articles from 1974 to 2020, divided into 9 categories, have been selected and used as reference in this paper (Figure 2A). The "diverse" category includes the articles with general themes close to the study, but which cannot fit into the other specified categories. Two thirds of the selected peer-reviewed articles are about SRS, with a majority of them specifically focusing on Landcover & vegetation and surface water (Figure 2A). We observed an increase in publications related to SRS since the early 2000s and a steady frequency of peer-reviewed articles focusing on buffalo and cattle (Figure 2B).

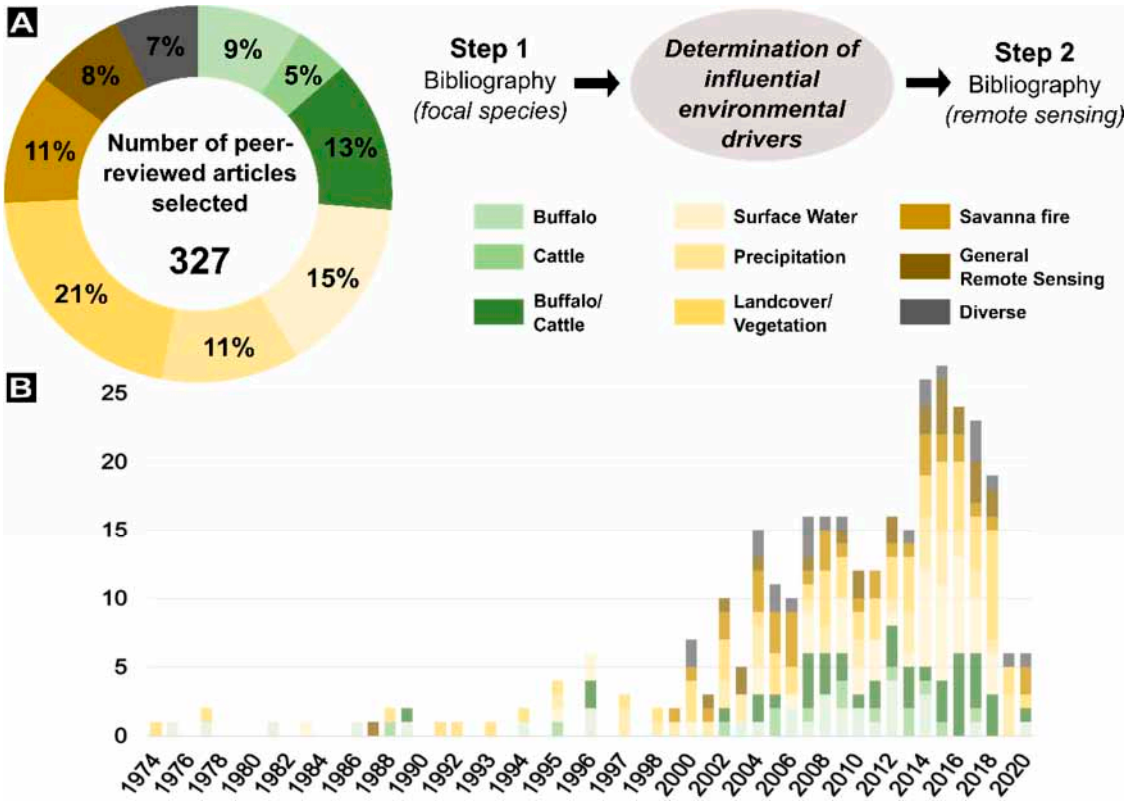

Figure 2. Statistics and chronology of the article bibliography by topic category. (**A**) The ring diagram represents the percentage of each category in relation to the total number of reviewed articles. (**B**) The horizontal axis of the histogram corresponds to the published year of the selected articles. The vertical axis corresponds to the number of published articles according to their respective categories.

3. Environmental Drivers Influencing the Movements of Buffalo and Cattle and the Satellite Remote Sensing Tools to Characterize them

The main environmental drivers (Landcover/vegetation, surface water, savanna fire and precipitation) identified through the reviewing process (Section 2) are illustrated through this section using the example of a buffalo/cattle interface localized in HNP, Zimbabwe (Figure 3). In this particular context, the two focal species interact at the interface between a national park and an adjacent CL (Figure 3A) where habitats cover a wide variety of environments and natural resources.

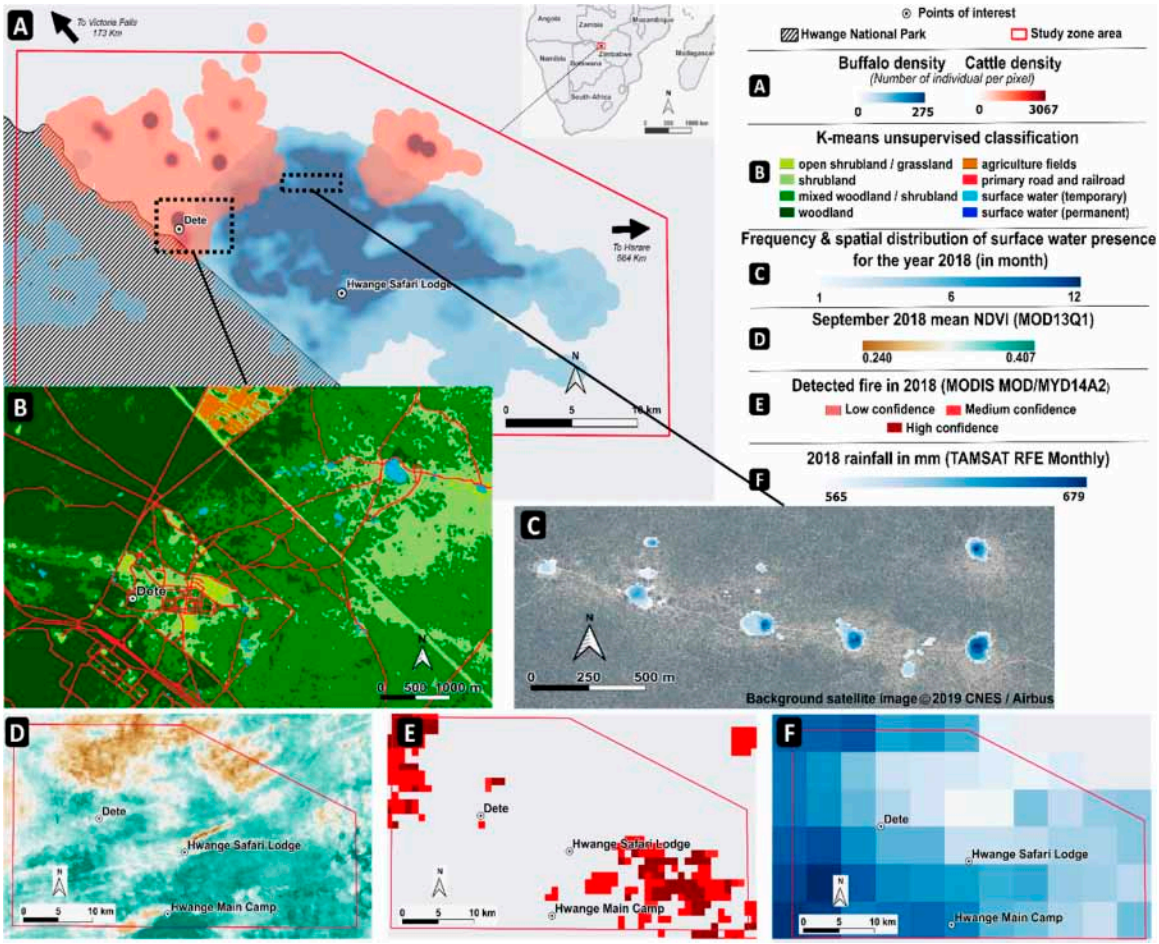

Figure 3. Illustrative examples of SRS-derived environmental drivers of buffalo and cattle movement in HNP, Zimbabwe (refer to supplementary materials for a complete description of the data used). (**A**) Map of the buffalo and cattle density based on GPS data set for both species (number of individual per pixel in the HNP interface ecosystem at 5m spatial resolution) [12]. (**B**) K-means unsupervised landcover classification map of Dete municipality next to HNP derived from Sentinel-2 imagery with a 10 m spatial resolution [61]. (**C**) Frequency and distribution of surface water presence at 10 m spatial resolution obtained via the Random Forest (RF) algorithm applied on a sentinel-2 image of March 2018 after the application of atmospheric corrections [61]. (**D**) Normalized Difference Vegetation Index (NDVI) map with a 250 m spatial resolution from the Moderate-Resolution Imaging Spectroradiometer (MODIS). (**E**) Map of fire detected in 2018 using the MOD14A2 Fire product with a 1 km spatial resolution. (**F**) Map of the yearly precipitation estimations by the Tropical Applications of Meteorology using SATellite data (TAMSAT V3.0) product with a 4 km spatial resolution [62,63].

3.1. Landcover

3.1.1. How Landcover and Vegetation Influences Cattle and Buffalo Movements

Landcover (cropland, forest, surface water, artificial cover, bare soil, human infrastructures, . . .) affects animal movements because it reflects differences in resource availability, habitat structure preferences and ease of travel [64–66]. Buffalo and cattle are ruminants and predominantly grazers [67–69]. They are associated with open environments, where grass species are more abundant [70], and the spatial and temporal variability of fodder resource drives the foraging responses of both species [71]. Seasonal shifts in the composition of their diet are common due to the availability of grass species [72,73]. During the dry season, i.e., when quantity and quality of food resources decrease, buffalo and cattle adopt a selective and opportunistic switching between different

types of habitat or concentrated feeding close to water sources [72,74]. Buffalo tend to avoid areas used by cattle due to strong dietary overlap [75,76], the presence of human activities, and can travel long distances to find suitable feeding resources during the dry season [71,77]. During the wet season, buffalo tend to select available feeding resources located close to watering points, limiting their daily travelled distances [70]. Cattle can range further away from their enclosures on their own, sometimes into protected areas in search of quality forage when the season is dry and when there is no fences surrounding the park [78]. In contrast, during the wet season, cattle focus on accessible and available shrub vegetation or low lying herbaceous vegetation at proximity of their respective enclosure and inside natural park in some instance [37]. Cattle are however prevented to enter agricultural fields during the growing season [79].

3.1.2. SRS Basics for Characterizing and Classifying Landcover

SRS is widely used to assess landcover [80–84]. Different types of satellite sensors (Table 1) record the electromagnetic radiations which characterize the landcover, may this be the radiation reflected (optical sensors), the radiation emitted (thermal infrared and passive microwave sensors) or the radiation scattered (active radar sensors) [85]. Their characteristics (spatial resolution, revisit time period, spatial coverage, data availability, spectral resolution—see Table 1) define their capacities to map different land cover types on a given study area.

Table 1. Small subset of Earth observation satellite systems allowing data acquisition that can potentially be used in the field of animal movement ecology.

Optical Remote Sensing Satellites							
Sensor Resolution	**Satellite**	**Spatial Resolution**	**Revisit Time Period**	**Nb of Spectral Bands**	**Access**	**Data Availability**	**Used in Buffalo/Cattle Ecological Studies**
Low Resolution	NOAA	1.1 Km Bands 1–2	2 times a day	5	Open-source	1978–present	[86,87]
	MODIS	250 m/bands 3–7 500 m/bands 8–36 1 km	2 times a day	36	Open-source	1999–present	[29,54,67,79, 87–89]
	Suomi NPP	Bands I1-5 375 m/bands M1-16 750 m	2 times a day	22	Open-source	2012–present	-
	Envisat MERIS	300 m	3 days	15	Open-source	2002–2012	-
	Sentinel-3	300 m	2 days	21	Open-source	2016–present	-
Medium Resolution	Landsat	Pan* 15 m/MS* 30 m/TIR* 60 to 100 m	16 days	4–11	Open-source	1972–present	[11,37,88,90]
	Sentinel-2	VNIR* 10 m/SWIR* 20 m/ACB* 60 m	5 days	13	Open-source	2015–present	[91]
	Aster	VNIR 15 m/SWIR 30 m/TIR 90 m	16 days	14	Open-source	1999–present	-
High Resolution	Spot	Pan 1.5 to 2.5 m/MS 6 to 10 m	26 days	4–5	Licensed	1986–present	[26]
	Ikonos	Pan 1 m/MS 4 m	1.5–3 days	5	Licensed	1995–2015	[54,92]
	Rapideye	MS 5 m	1–5.5 days	5	Licensed	2008–present	[26]
	ZY-3	Pan 2.1 m/MS 5.8 m	5 days	4	Licensed	2012–present	-
	GF-1/GF-2	MS 5 m	4–5 days	5	Licensed	2013–present	-
	Planetscope-DOVEs	MS 3 m	Daily	4	Licensed	2017–present	-
Very-high Resolution	Quickbird	Pan 0.61 m/MS 2.24 m	2.7 days	5	Licensed	2001–2015	-
	WorldView	Pan 0.31 m/MS 1.24 m	1–4 days	4–17	Licensed	2007–present	[79]
	Geoeye	Pan 0.41/MS 1.64 m	3 days	5	Licensed	2008–present	-
	Pleaides	Pan 0.7 m/MS 2.8 m	Sub-daily	5	Licensed	2011–present	-
	Skysat	Pan 0.9 m/MS 2 m	Sub-daily	5	Licensed	2013–present	-

Table 1. *Cont.*

Radar Remote Sensing Satellites							
Satellite	**Frequency**	**Spatial Resolution**	**Revisit Time Period**	**Polari-zation**	**Access**	**Data Availability**	**Used in Buffalo/Cattle Ecological Studies**
ERS-1/ERS-2	C-band (5.3 GHz)	30 m	35 days	VV	Open-source	1991–2001	-
Radarsat 1	C-band (5.3 GHz)	50 m	24 days	HH	Open-source	1995–present	-
Radarsat 2	C-band (5.405 GHz)	25 m	24 days	VV-VH	Licensed	2007–present	-
Envisat ASAR	C-band (5.3 GHz)	12.5 m	35 days	VV	Open-source	2002–2012	-
TerraSAR-X/TanDEM-X	X-band (9.6 GHz)	5 m	11 days	HH-VV	Licensed	2007–present	-
Sentinel-1	C-band (5.405 GHz)	FR* 3.5 m/HR* 10 m and 25 m/MR* 25 m and 40 m	6 days	VV-VH	Open-source	2014–present	-
Alos PALSAR 1-2 Alos PALSAR 2	L-band (1.27 GHz)	SP* 9 × 10 m/DP* 19 × 10 m	46–14 days	VV VH HH HV	Licensed	2006–present	-

* Visible Near Infrared (VNIR)/Short-wave Infrared (SWIR)/Thermal Infrared (TIR)/Atmospheric Correction Bands (ACB)/Panchromatic (Pan)/Multi-spectral (MS)/Full Resolution (FR)/High Resolution (HR)/Medium Resolution (MR)/Single Polarization (SP)/Dual Polarization (DP).

Two main categories of classification methodologies are commonly used in SRS to produce landcover maps. Supervised classification methodologies use different machine learning algorithms (maximum likelihood, neural network ensembles, random forests (RF), ...) to discriminate user-determined landcover categories [93]. For example, the RF algorithm uses a set of decision trees [94] and is now widely used [95,96], with the advantages of reliable and rapid execution in processing time of large volume of variables and data [97,98]. Such approaches require the definition of a training dataset of the different classes to be distinguished before classification. On the other hand, unsupervised classifications methodologies are more automatic processes, relying on algorithms such as K-means or Agglomerative Hierarchical to discriminate landcover categories [99]. The two types of classification methods can be applied to classify either image pixels, based on their spectral or textural values, or objects, i.e., neighboring pixels with similar spectral values aggregated into "objects" prior to the classification process. In the latter case, additional object-specific features such as shapes, context features/neighborhood relation, scale-hierarchy relation can be used to characterize and classify the objects [100]. In all cases, ground-truthing data are required for accuracy assessment.

Optical satellite images such as MODIS and Landsat (Table 1) have been used extensively for land cover classification since the 1970s and have enabled the dissemination of freely available landcover map products (Table 2) that represent major landscape features on a global scale. These products provide an initial characterization of landscape features that can be useful considering landcover preliminary assessments in a particular study area and can be easily operated by users with little SRS knowledge. The recently launched ESA-S2-LC20 product (Table 2) is one good example and can fulfil such a task despite a moderate accuracy [101]. However, as their spatial resolution and typologies are possibly not adapted to the study of ungulates habitats, 'customized' landcover maps can be produced to better reflect the landscape complexity of a particular study area [102]. Implementing optical indexes of vegetation, soil (Table 3) and water (Table 4) can also potentially enhance landcover classification results [103,104].

Despite high capacities to produce landcover maps, optical satellite images are not without limitations (e.g., lack of cloud-free periods) [105] and synthetic aperture radar (SAR) images (Figure 4 and Table 1) can provide a reliable alternative to optical satellite images. SAR sensors produce their own source of illumination and therefore can operate in almost any weather condition, day or night, and penetrate different types of vegetation cover [106,107]. They have shown good results to classify landcover in general [108], forests [109] and biomass [110] in particular and are, as a result, increasingly used. Several studies have demonstrated the complementarity of SAR and optical data and concluded that using them together provides better results than using them separately [22,111,112], especially in tropical environments where the cloud coverage often hinders the use of optical satellite images [113].

Table 2. List of satellite remote sensing-based landcover products.

Product Name	Spatial Resolution	Data Availability	Sensor Used	Reference
Climate Change Initiative (CCI) LandCover V2	300 m	1992 to 2015–2016–2017–2018	MERIS Full and Reduced resolution/Spot VGT	[114]
MCD12Q1 0.5 km MODIS-based Global LandCover	500 m	2001–today	MODIS	[115]
Globeland30	30 m	2000/2010	Landsat TM, ETM7, HJ-1A/b	[116]
GLC 2000	1 km	2000	SPOT 4 VEGETATION	[117]
GlobCover 2005 V2.2 2009	300 m	2005/2009	MERIS FR	[118]
GLCNMO V.1-V.2-V3	1 km/500 m	2003/2008/2013	MODIS	[119]
GLC Share	1 km	2014	MERIS-MODIS	[120]
GLC250 m CN (2001/2010)	250 m	2001/2010	MODIS	[121]
FROM-GLC (GLC, GLC-seg, GLC-agg, GC, GLC-hierarchy)	30 m	2010	Landsat TM, ETM+	[122]
Global 30m Landsat Tree Canopy (TCC) V.4	30 m	2000, 2005, 2010, and 2015	MODIS, Landsat TM, ETM+	[123]
Global Forest Change (GFC) - GLAD (Global Land Analysis & Discovery) lab at the University of Maryland (UMD)	30 m	2000 to 2019	Landsat TM, ETM+, OLI	[80]
Copernicus Global 100 m Landcover (CGLS-LC100)	100 m	2015	PROBA-V EO and GSD	[124]
ESA-S2-LC20, 20 m (over Africa)	20 m	2016	Sentinel-2A	[125]

3.1.3. SRS for Detecting Landcover and Vegetation Changes

Detection of landcover changes is a complicated and integrated process and there is no optimal and applicable approach to all cases [126]. Several studies have demonstrated the capacity of Landsat images, which offer the longest continuous record of medium-resolution satellite-based earth observation (Figure 4), to monitor long term environmental changes in savanna environments [127,128]. Optical remote sensing sensors allow to monitor the evolution of the vegetation through phenology based on the spectral signature of vegetation [129,130]. For example, the widely used normalized difference vegetation index (NDVI) (Table 3) [131] was demonstrated highly correlated with the vegetation photosynthetic activity [132–134], vegetation development and seasonal patterns, forage cumulative growth period quality and quantity assessments [135–137]. These properties allow monitoring and comparing vegetation phenology through space and time at different scales. The Figure 3D, for example, represents one image (month of September 2018) of the MODIS MOD13Q1 NDVI time series, giving a spatial representation of the vegetation repartition across the HNP interface area.

NDVI was also found correlated with animal movements [138,139]. However, in savanna environments, the relevance of simple indexes such as the NDVI can be limited and must be used with caution. Using low spatial resolution satellite sensors (i.e., MODIS) or even medium resolution satellite sensors (i.e., Landsat or Sentinel-2), pixels are most of the time mixed pixels of varying proportion of trees, grasses and bare soil [140,141]. In that case, the use of soil-adjusted vegetation indexes (Table 3) may be used as complementary to enhance classification results and seasonal analyses of landcover evolution [142,143] when applied within the frame of animal movement studies.

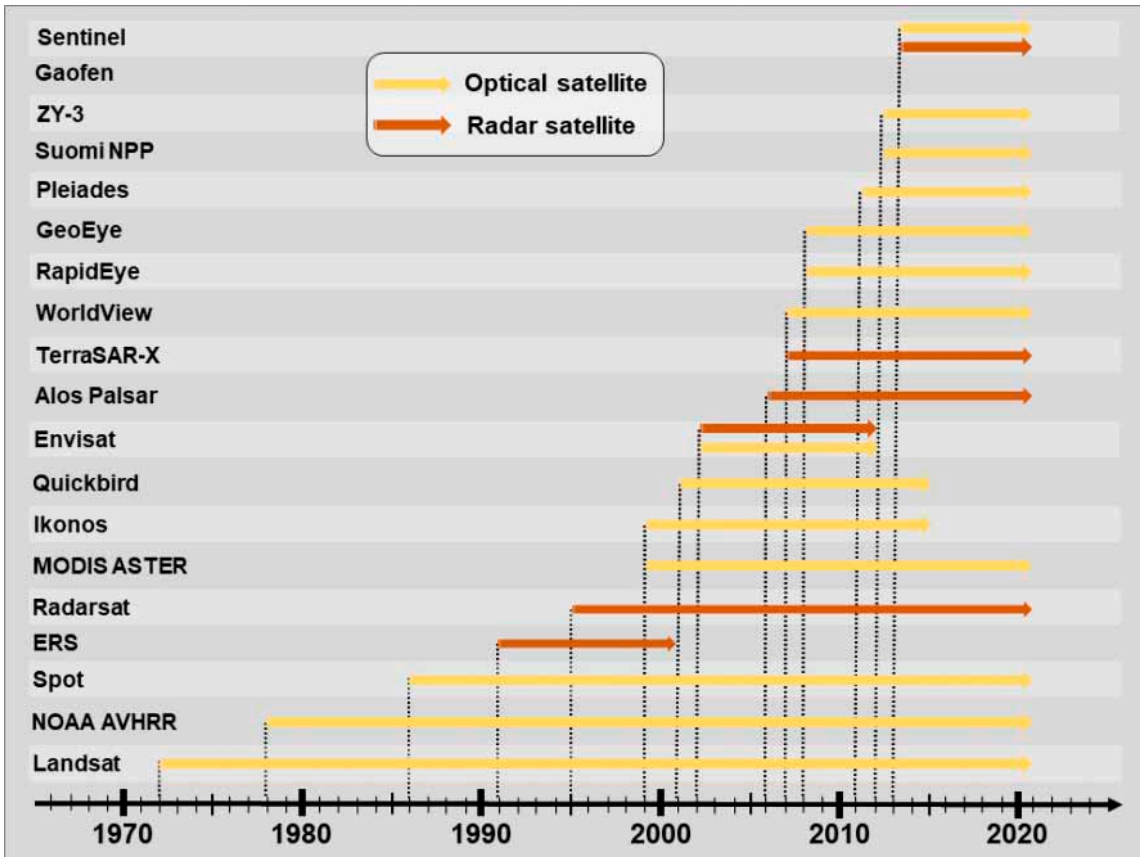

Figure 4. Earth observation optical and radar satellites commissioning and time of service chronology. The length of the arrow represents the continuity and the duration of the corresponding satellite program.

3.1.4. SRS to Characterize Landcover and Vegetation When Studying Animal Movements in Savanna Environments

Applying landcover classification to a savanna landscape can be challenging due to sparse cover, high background soil signal, and difficulty to differentiate between spectral signals of bare soil and dry vegetation [144]. Despite these limitations, Arraut et al. (2018) produced a map of the vegetation structure of HNP in seven classes using 2013–2014 Landsat satellite images through a supervised classification process with an overall accuracy (OA) of 83.2% [102]. Figure 3B presents another example of a landcover map derived from an unsupervised classification (K-means algorithm) applied to a Sentinel-2 satellite image.

Such tailored SRS landcover maps have been used in different studies of buffalo and cattle ecology aiming at relating animal movements and landcover (Table 1). For example, Cornélis et al. (2011) used a sylvo-pastoral vegetation map derived from 30 m resolution Landsat imagery to investigate the habitat preferences of buffaloes in W Regional Park (Burkina Faso, Benin, Niger) [88]. At local scale, very high spatial resolution sensors such as Worldview-2 and IKONOS were used (Table 1) to produce fine-scale landcover maps allowing the determination of resource use of cattle in communal lands in South Africa [79] and Zimbabwe [92].

Vegetation indexes (Table 3) provide a synthetic description of the vegetation spatio-temporal dynamics and several studies have related SRS derived vegetation indices such as the NDVI or the Enhanced Vegetation Index (EVI) (Table 3) to the spatio-temporal distribution and abundance of buffalo and other ungulates species at different scales [26,29,54,68,79,86,88,89,145–147]. For example, Naidoo et al. (2012a) used MODIS EVI time series to measure the greenness of the vegetation and demonstrated the importance of this variable in explaining the variations in home range size of buffaloes in northeastern Namibia [29]. In two Australian savanna study sites, Handcock et al. (2009) showed

that the tracks of cattle from GPS collars overlaid with a NDVI map derived from a 10 m resolution SPOT-5 image, highlighting a correlation between NDVI and cattle movements [26]. Using very high spatial resolution imagery, Zengeya et al. (2015) derived a fine scale EVI map from an IKONOS image to determine the proportion of cattle home range observed inside and outside a conservation area [54].

Table 3. Non-exhaustive list of spectral remote sensing indexes developed to discriminate vegetation and soil from optical satellite image analysis and that can be useful within the frame of animal movement studies in savanna environments.

Spectral Index	Calculation *	Reference	Used in Buffalo/Cattle Ecological Studies
Normalized Difference Vegetation Index (NDVI)	$(NIR - RED)/(NIR + RED)$	[148,149]	[26,68,79,86,88,145–147]
Enhanced Vegetation Index (EVI)	$2.5 \times [(NIR - RED)/((NIR + 6 \times RED - 7.5 \times BLUE) + 1]$	[150]	[29,54,89,146]
Global Environmental Monitoring Index (GEMI)	$n = [n \times (1 - 0.25 \times n) - (RED - 0.125)]/1 - RED$ $\left[2 \times \left(NIR^2 - RED^2\right) + 1.5 \times NIR \times 0.5 \times RED\right]/NIR + RED + 0.5$	[142]	-
Soil Adjusted Vegetation Index (SAVI)	$[(1 + L) \times (NIR - RED)]/NIR + RED + L$ $L = 0.5$	[143]	-
Modified Soil Adjusted Vegetation Index (MSAVI)	$[2 \times NIR + 1 - \sqrt{(2 \times NIR + 1)^2 - 8 \times (NIR - RED)}]/2$	[151]	-
Modified Secondary Soil-Adjusted Vegetation Index (MSAVI2)	$0.5 \times [2 \times NIR + 1) - \sqrt{(2 \times NIR + 1)^2} - 8 \times (NIR - RED)]$	[152]	-
Difference Vegetation Index (DVI)	$NIR - RED$	[153]	-
Optimized Soil-Adjusted Vegetation Index (OSAVI)	$(1 + Y \times [(NIR - RED)/(NIR + RED \times Y)]$ *where* $Y = 0.16$ (*optimal value*)	[154]	-
Soil Brightness Index (SBI)	$0.30372 \times BLUE + 0.27933 \times GREEN + 0.47434 \times RED +$ $0.55858 \times NIR + 0.508210 \times SWIR + 0.186312 \times MIR$	[155]	-
Two-band Enhanced Vegetation Index (EVI2)	$2.4 \times (NIR - RED)/(NIR + RED + 1)$	[156]	-
Modified Chlorophyll Absorption Ratio Index (MCARI)	$[(VNIR - RED) - 0.2 \times (VNIR - GREEN)] \times (VNIR/RED)$	[157]	-

* BLUE, GREEN, RED, NIR, MIR, SWIR: reflectance values in blue, green, red, near infrared, mid infrared and short-wave infrared, respectively. VNIR (visible and near infrared), SWIR1 ad SWIR2: reflectance values from bands 5, 11 and 12 of Sentinel-2 respectively.

3.2. Surface Water

3.2.1. How Surface Water Distribution Influences Cattle and Buffalo Movements

The availability of surface water, artificial (e.g., solar-pumped, diesel generator) [158] or natural (e.g., dams, rivers) [159], is commonly cited to constrain movements and space-use of herbivores, including savanna buffalo [88,160–163] and cattle [164,165]. However, the influence of water sources in herbivore distributions is expected to change in response to variations in forage quality and quantity [166,167]. Buffalo are usually associated with areas close to water all-year-round and drink every day [90,168,169]. Similarly, cattle preferentially select areas close to water points, usually around their enclosures in order to optimize the ratio of energy expenditure to energy gain [79,170] and can also use boreholes which are never accessible to buffalo [90].

3.2.2. SRS Basics for Detecting Water and Water Dynamics

Optical SRS imagery can be efficient to discriminate water surface in different environments due to a wide range of sensors (Figure 4 & Table 1) with various spatial and temporal resolutions available [171–176]. Depending on surface water properties (i.e., size, river, pond, seasonal) to detect, different categories of sensors can be chosen [177]. However, their spatial resolution may affect their efficiency in accurately detecting surface water.

Many methodologies, from thresholding a single infrared band to the use of multi-spectral classification decision trees, have been developed to detect surface water via SRS [178–180]. They rely on the spectral signature of water, characterized by a quick reduction of reflectance from the blue to the near infrared wavelengths. Water indexes based on two or more spectral bands calculation (Table 4) and various spectral band combinations have been widely used to detect surface water [181,182] (see example in Figure 3C).

Other factors should also be considered as they potentially limit the satellite-based detection of surface water extent [183]: water depth, water turbidity variation, soil characteristics, vegetation cover, potential cloud cover and shadows. They all influence the water reflectance whatever the spatial resolution of the satellite images and influence thresholding values and the efficient use of water indexes. Despite these constraints, accurate methodologies can be developed to discriminate water by adding complementary spatial information to spectral indexes alone. Owen et al. (2015) for instance, have been able to accurately detect artificial waterholes across heterogeneous desert environments using Landsat 8 data combined with spectral indexes and texture analysis [184].

Table 4. Non-exhaustive list of spectral remote sensing indexes developed to discriminate water surfaces from optical satellite image analysis and that can be useful within the frame of animal movement studies in savanna environments.

Spectral Index		Calculation*	Reference
Normalized Difference Infrared Index	NDII	$(NIR - MIR)/(NIR + MIR)$	[185]
Normalized Difference Vegetation Index	NDVI	$(NIR - RED)/(NIR + RED)$	[148,149]
Enhanced Vegetation Index	EVI	$2.5 \times [(NIR - RED)/(NIR + 6 \times RED - 7.5 \times BLUE + 1)]$	[150]
Normalized Difference Water Index	NDWI	$(GREEN - NIR)/(GREEN + NIR)$	[186]
Normalized Difference Water Index (Gao)	NDWI (Gao)	$(GREEN - SWIR)/(GREEN + SWIR)$	[187]
Modified Normalized Difference Water *Index*	MNDWI	$(GREEN - MIR)/(GREEN + MIR)$	[188,189]
Normalized Difference Turbidity Index	NDTI	$(RED - GREEN)/(RED + GREEN)$	[188]
Normalized Difference Phytoplankton Index	NDPI	$(MIR - GREEN)/(MIR + GREEN)$	[188]
Automated Water Extraction Index	AWEInsh AWEIsh	$\text{AWEInsh} = 4 \times (GREEN - SWIR1) - (0.25 \times NIR + 2.75 \times SWIR2)$ $\text{AWEIsh} = BLUE + 2.5 \times GREEN - 1.5 \times (NIR + SWIR1) - 0.25 \times SWIR2$	[190]
Water Index	WI	$1.7204 + 171 \times \text{GREEN} + 3 \times \text{RED} 70 \times \text{NIR} 45 \times \text{SWIR}171 \times \text{SWIR}2$	[191]

* BLUE, GREEN, RED, NIR, MIR, SWIR: reflectance values in blue, green, red, near infrared, mid infrared and short-wave infrared, respectively. VNIR (visible and near infrared), SWIR1 and SWIR2: reflectance values from Bands 5, 11 and 12 of Sentinel-2, respectively.

Synthetic aperture radar (SAR) satellite images can be used independently or in combination with optical satellite images in order to detect surface water [192,193]. The recent increase in number of operational SAR sensors (Table 1 & Figure 4) has favored their use for surface water detection. Indeed, several SAR-based water detection methodologies have been developed such as the surface water detection through supervised and unsupervised classifications [194,195], thresholding [196,197], object-based image analyses [198,199] and hybrid approaches [200,201]. The application of these different methodologies led to the development of several surface water products (Table 5) [202–205].

The accuracy of the SAR-based surface water detection methodologies varies. Terrain shadowing due to the topography can result in a side-looking effect [197]. The importance of the vegetation layer can produce double-bounce scattering of the signal that increases the backscatter measured in the SAR image [206]. The strong wind that roughens the water surfaces can lead to misclassification errors and the threshold value to discriminate the surface water is dependent of the image quality acquisition and the type of landscape [193]. Nevertheless, surface water long-term monitoring has been successfully implemented in a savanna environment via a multi-SAR-system at high and very-high spatial resolution [207].

3.2.3. SRS to Detect Surface Water When Studying Animal Movements in Savanna Environments

SRS-based water products like the Global Surface Water (GSW) and the Global Water Body map (G3WBM/G1WBM) present the advantage to have a higher spatial resolution and temporal frequency compare to the other products listed in Table 5. These products are suitable to detect massive bodies of water at a continental scale and can be of interest for preliminary analyses, however they show strong limitations when trying to discriminate localized, small or seasonal surface water which are predominant in savanna environments [208]. Indeed, detecting surface water in savanna environments via remote sensing at a landscape scale remains challenging mostly because of surface water seasonality dynamics, landscape heterogeneity and variety in surface water area sizes and morphologies [208,209].

Increasing availability of free medium-resolution optical and radar satellite sensors such as Sentinel-1 and Sentinel-2 (Table 1) offers potentialities to accurately discriminate, via supervised classification, surface water and surface water dynamics [210]. Among the different spectral remote sensing indexes developed to discriminate water surface from optical satellite images (Table 4), the MNDWI and NDWI are the most commonly used [211] and were identified as efficient discriminating indexes for the detection of surface water extent in savanna environments [177,212]. In the case of the HNP study area shown in Figure 3C, a time series of 12 Sentinel-2 images (one image per month for the year 2018) combined with the application of the RF algorithm on MNDWI and NDWI indexes (Table 4) was used to characterize the presence and seasonal dynamics of the surface water.

So far, water spectral indexes in combination with supervised classification have hardly been used in direct relation with buffalo and cattle movements, although their potential within this framework have already been stressed [212]. Recently, Naidoo et al. (2020) used the NDWI calculated from Sentinel-2 images to detect ephemeral water source in relation with buffalo and elephant movements in Namibia [91]. However, most of the reviewed studies integrating water into their analysis only used on-site observations of surface water [88,147,167] and natural or artificial waterholes [17,213–216].

Table 5. Non-exhaustive list of remote sensing-based water products.

Product Name	Developer	Spatial Resolution	Frequency	Data Availability	Reference
Global surface water (GSW)	EC JRC (European Commission Joint Research Center)/Google	30 m	Monthly Yearly	1984–2015 1984–2019	[217]
CCI global map of open water bodies (WBP V4.0)	ESA (European Space Agency) - climate change initiative(CCI)	300 m to 1 km	7 days–1 year	2000–2015	[218]
Global lakes and wetlands database (GLWD)	University of Kassel/World Wildlife Fund (WWF)	1 km	1 year	2004	[219]
SRTM water body data product specific guidance (SWBD)	National Aeronautics and Space Administration (NASA)	90 m	1 year	2000	[220]
SAR-Based water body indicator (SAR-WBI)	ESA	150 m to 1 km	6 to 12 days	2005–2012	[221]
MOD44W	NASA	250 m	yearly	2000–2015	[222]
Copernicus WB	Copernicus program-ESA	300 m to 1 km	10 days	2014–present	[223]
Global 3-s/1-s water body map (G3WBM/G1WBM)	Department of Integrated Climate Change Projection Research, 4 Japan Agency for Marine-Earth Science and Technology	30 m to 90 m	1 year	2018	[224]

3.3. Fire Regimes

3.3.1. How Fire Influences Cattle and Buffalo Movements

Savanna is prone to fire due to the existence of a highly flammable continuous vegetation layer with ideal burning conditions during the dry season [225,226]. Savanna fires can thus affect herbivores movements, by impacting indirectly the quantity and quality of the grazing resources available **[227]** or by reducing cover to hide from predation [228]. Although most herbivores are attracted to the recently burned areas due to nutritious regrowth [229], buffalo habitat selection during the dry season appear to be strongly constrained by the occurrence of fire, probably due to a great reduction of the quantity of forage [75]. Fire can also affect the migration distance of buffalos during the wet season [146].

Movement patterns of cattle are also influenced by the occurrence of fire. In Kenyan savanna ecosystems, prescribed burning improved cattle forage intake but only in areas that cattle did not share with wildlife [230]. Savanna fires could, therefore, affect livestock-wildlife coexistence at the interfaces by altering the intensity and frequency of forage use [229].

3.3.2. SRS Basics for Detecting Fire and Fire Dynamics

Optical SRS can be used to spatially and temporally detect and characterize burnt area and burn severity [231–233] based on the detection of changes in the spectral signatures of vegetation [234] with a reflection reduction in the visible and near infra-red (NIR) spectral bands. Indeed, the charring and removal of vegetation are largely visible and detectable in the infrared [235].

Various SRS-based approaches have been developed to monitor fire [236,237], including aggregate active detection [238,239], multi-temporal composites analyses [240], the use of spectral indexes [241], including vegetation indexes such as NDVI or GEMI (Table 3), spectral mixture analysis [242], machine learning classification [243,244], time series change detection [245] and hybrid approaches mixing time series change detection with machine learning classification [246,247]. If these methods provide user friendly fire products (Table 6) and helpful fire spectral indexes (Table 7) by capturing most aspects of

the spatial and temporal distribution of the fire effects, it can be difficult to relate them to actual burned area due to inadequate spatial and temporal resolutions, variability in cloud cover and differences in fire behavior [248]. Active fire detection algorithms may either: (i) underestimate the area burned in grassland and savanna ecosystems as the fire progresses rapidly across the landscape [249] and because small and low-intensity fires may not be detected [250]; (ii) overestimate the burned area for isolated fire points smaller than the pixel dimension [250]. In this instance, the MODIS fire products MOD14A2/MYD14A2 and MCD45A1 (Table 6) provide three categories of confidence (low, medium, high) of fire detection (Figure 3E), offering flexibility for a targeted use in accordance with the user's choice.

3.3.3. SRS to Characterize Fire when Studying Animal Movements in Savanna Environments

The Figure 3E shows an example of the MODIS fire product MOD14A2 (Table 6) at the HNP interface, illustrating the capacity of such product to depict with a 1km spatial resolution the active fire temporal and spatial dynamics and its potential for conducting seasonal- and inter-annual analyses. Despite the availability of numerous SRS-based fire products offering a wide range of applications (Table 6), according to our review only one of them has been used in relation with buffalo and cattle movement studies. Naidoo et al. (2012b) used the MODIS MOD14A2/MYD14A2 product to quantify the relative effect of dry season variables, including savanna fires, on subsequent wet season buffalo migration distance in a large study area running east-west between the northeast corner of Namibia, Angola and Botswana [146].

As shown by this example, and despite limitations, the data listed in Table 6 presents the advantage to describe fire phenomenon in relation with animal distribution and movement in regions with scarce fire information [251]. In well-documented areas, these data can potentially be used to complement existing fire databases. Combining better spatial resolution from new sensors such as Sentinel-3 (Table 1) and remote sensing-based fire products with designed spectral indexes to detect fire (Table 7) is promising. It could potentially reduce errors and uncertainties in satellite-derived fire dates and ignitions, and improve coverage of small fires. The recently launched FireCCI50 product (Table 6) offers an increased spatial resolution (250 m) and a better burned area estimation compared to the MODIS fire products [249]. This spatial resolution could be useful when aiming to integrate fire assessment in animal movement study at the landscape scale in savanna environments.

Table 6. Non-exhaustive list of satellite remote sensing-based fire products.

Product Name	Spatial Resolution	Orbital Frequency	Data Availability	Reference	Use in Ungulates Ecological Studies
MOD14A2/MYD14A2	1 km	Every 8 days	2000–present	[252]	[29]
MCD45A1	500 m	Monthly	2000–present	[253]	-
MCD64A1	500 m	Monthly	2000–present	[248]	-
VIIRS 750 m active fire (VNP14)	750 m	twice/day (IR and day/night VIS/NIR channel) once/day (VIS)	2011–present	[254]	-
VIIRS 375 m Active Fire (VNP14IMG)	375 m	twice/day (IR and day/night VIS/NIR channel) once/day (VIS)	2016–present	[238]	-
Sentinel-3 SLSTR (level-2 FRP product)	1 km	Daily	2018–present	[255]	-
AVHRR Fire Detects from the Fire Identification, Mapping and Monitoring Algorithm (FIMMA)	1 km	Daily	1978–present	[256]	-
ESA FIRE_CCI	300 m	Monthly	2016–present	[257]	-
FireCCI51	250 m	Monthly	2001–2019	[258]	-

Table 7. Non-exhaustive list of spectral remote sensing indexes developed to discriminate fire from optical satellite image analysis and that can be useful within the frame of animal movement studies in savanna environments.

Spectral Index	Calculation *	Reference
Normalized Burned Ratio (NBR)	$(NIR - SWIR)/(NIR + SWIR)$	[258]
Burned Area Index (BAI)	$1/(NIR - 0.06)^2 + (RED - 0.1)^2$	[259]
Mid Infrared Burned Index (MIRBI)	$10 \times SWIR + 9.8 \times SWIR + 2$	[260]
Char Soil Index (CSI)	$NIR/SWIR$	[261]
Normalized Burn Ratio Thermal (NBRT)	$(NIR - SWIR \times TIR)/(NIR + SWIR \times TIR)$	[262]
Normalized difference Vegetation Index Thermal (NDVIT)	$(NIR - RED \times TIR)/(NIR + RED \times TIR)$	[262,263]

* RED, NIR, MIR, SWIR, TIR: reflectance values in red, Near Infrared, Mid Infrared, Short-wave Infrared and Thermal Infrared, respectively.

3.4. Precipitation

3.4.1. How Precipitation Influence Cattle and Buffalo Movements

In southern African savannas, the availability in time and space of natural resources (i.e., surface water and forage) is strongly dependent of the precipitation seasonal variations [88,264]. Most precipitation occurs during the wet season (November to April). However, the spatio-temporal distribution of precipitations in southern Africa is highly heterogeneous at medium-scale inducing specific movement patterns such as nomadism [265]. During the dry season (May to October), precipitation are lower or nonexistent, and the availability of natural resources decreases. This high heterogeneity in rainfalls dictates the behavior of wildlife [8].

Buffalos, like other ungulates of semi-arid savannas, are able to track precipitation events over large distances [88]. Buffalos living in wetter areas, such as in forested savanna habitats, tend to maintain smaller and constant home ranges than those in drier open savanna habitats [160,266]. In these more arid areas, natural resources are spatially unevenly distributed, forcing buffalos to travel longer distances in their search for forage and water [29,146,162]. In some areas however, smaller buffalo home ranges have been noticed during the dry season compared to the wet season [266–268].

Precipitation also affect cattle movement patterns through the combined influence on their grazing behaviors and the spatial grazing constraints imposed by livestock owners [269]. For example, cattle around Kruger National Park, South Africa, select forage with higher quantity and quality during the dry season but behave more like non-selective bulk grazers during the wet season, directly influencing their daily traveled distance [79].

3.4.2. SRS Basics for Measuring Precipitation

Satellite-based precipitation measurements with advanced infrared (IR), passive microwave (MW) and radar (SAR) sensors provide a complementary alternative to in-situ records [62,270] as they give a full spatial and temporal coverage with a good accuracy (Table 8) [271–278]. Yet, despite the growing collection of satellite-based rainfall measurement datasets providing near-real-time estimates [63], only a few high-resolution satellite-based products providing historical data at the daily time-step with real-time or near-real-time updates for the African continent are publicly available (Table 8). To improve the accuracy of rainfall estimations, the merging of satellite and gauge measurements have been designed, thus maximizing the benefits of each data type [279,280]. Noticeable differences can be found in the performance of the satellite precipitation estimates though [281]. Satellite-based precipitation products generally overestmate precipitation events under 200 mm/month and tend to underestimate daily time scale precipitation events compare to the decadal and monthly time scale

precipitation events [272,282,283]. However, the main precipitation regimes and the spatial patterns of mean annual precipitation are well reproduced [281,284].

Satellite-based precipitation measurements have the advantage of providing full spatial coverage compared to the more accurate but spatially limited rain gauge data [285]. Furthermore, observational precipitation measurements over Africa include uncertainties that can bias analysis [286,287]. The TMPA 3B42 V7 (TRRM) offers the advantage of consistency at the daily time-scale [281]. It is a performing product for depicting inter-annual variations but offers a coarser spatial resolution (Table 8) which could be detrimental when studying animal movement at the landscape scale. Since 2019, the GPM IMERG v06 algorithm fuses the early precipitation estimates collected during the operation of the TRMM satellite (2000–2015) with more recent precipitation estimates collected during operation of the GPM satellite (2014–present). Therefore, the GPM IMERG v06 now offers 20 years of data coverage and can potentially be of interest regarding animal movement studies at the landscape scale regarding its spatial resolution of 0.1° and its broad coverage (Table 8).

The products that combine thermal infrared and passive microwave imagery such as RFE or CHIRPS (Table 8), perform comparatively well and outperform products which are only based on thermal infrared imagery such as TARCAT (Table 8) [272]. They could be used in complement or independently with higher spatial resolution satellite-based precipitation products such as the GPM product (Table 8) to reliably assess precipitation at the landscape scale in seasonal-prone environments such as African savannas when lacking in-situ precipitation data.

Table 8. Non-exhaustive list of available satellite-based precipitation products.

Product Name	Temporal Resolution	Spatial Resolution	Data Availability	Coverage	In-Situ Calibration	Reference	Use in Ungulates Ecological Studies
TRMM (TMPA 3B42 V7)	3 h	0.25°	1998–Mid 2019	50°S–50°N	yes	[288]	[29,146]
TRMM (TMPA 3B43 V7)	Monthly	0.25°	1998–Mid 2019	50°S–50°N	yes	[288]	[29,146]
PERSIANN-CDR	Hourly/Daily/ Monthly/yearly	0.25°	1983–present	60°S–60°N	no	[289]	-
GPCP (1dd)	Daily	1°	1996–present	90°S–90°N	no	[290]	-
GPCP V2.3	Monthly	2.5°	1979–present	90°S–90°N	no	[291]	-
CPC Global	Daily	0.5°	1979–present	90°S–90°N	yes	[292]	-
CMAP	Monthly	2.5°	1979–present	90°S–90°N	yes	[293]	-
Cmorph	30 min	0.25°	2002–2017	60°S–60°N	no	[294]	-
GPM (IMERG V06)	30 min/ 3 h/Daily	0.1°	2000–present	60°S–60°N	no	[295]	-
MSWEP V2	3 h/Daily	0.1°/0.5°	1979–2017	90°S–90°N	yes	[296]	-
SM2RAIN-ASCAT	Daily	0.5°	2007–2018	60°S–60°N	no	[297]	-
TAMSAT V3.1	Daily	0.0375°	1983–present	38°025N–35°9625S 19°0125W–51°975E	yes	[62,63]	-
CHIRPS v2p0	Daily	0.05°	1981–present	50°S–50°N	yes	[298]	-
ARC V.2	Daily	0.1°	1983–present	40°S–40°N	yes	[299]	-
RFE 2.0	Daily	0.1°	2001–present	40°S–40°N 20°W–55°E	yes	[300]	-
EPSAT-SG	15 min	0.0375°	2004–present	African continent	yes	[301]	-
MPE	15 min	0.0375°	2007–present	African & European continents	no	[302]	-

3.4.3. SRS to Measure Precipitation when Studying Animal Movements in Savanna Environments

Only the National Oceanic Atmospheric Administration (NOAA) African Rainfall Climatology (ARC V.2), the Climate Hazards Group InfraRed Precipitation with Station data version 2.0 (CHIRPS20) and the Tropical Applications of Meteorology using SATellite data and ground-based observations (TAMSAT V3.1) provide continually updated daily time-step data [63,303]. Therefore, due to their

spatial and temporal resolutions (Table 8) they are potentially suitable for applications in animal movement studies in African savanna environments. Figure 3F shows a spatial representation of the TAMSAT V3.1 at the HNP interface while demonstrating the product capabilities to detect spatially contrasted precipitation within a relative extensive area (1192 km^2). TAMSAT V3.1 (Table 8) is among the best product in terms of precipitation event detection at a spatial resolution of 0.0375° [304] but it may underestimate monthly rainfall measurements [284].

Despite the availability of these precipitation satellite-based products, the most commonly method to characterize precipitation in relation with animal movement and distribution remains the use of in-situ gauging stations data [170,305]. Only few studies have used satellite-derived precipitation data in relation with buffalo movements. Naidoo et al. (2012a, 2012b) used TRMM data (Table 8) to characterize which environmental factors, including precipitation, explain buffalo migration patterns [146], and variation in buffalo home range sizes in northeastern Namibia [29].

4. Discussion

The literature on the current knowledge on buffalo and cattle movements and their interactions was here linked to an inventory of available and relevant SRS tools to characterize the environmental drivers of these movements, found in savanna type landscape environment.

Landcover, surface water, savanna fire and precipitation emerged through this review as environmental drivers defining buffalo and cattle movements at the edge of protected areas in Africa and in southern Africa in particular. Optical and radar SRS are both currently operational to characterize these drivers and have already been used independently for several ecological applications, including animal movements [19,25,306] but have never been collectively linked in animal movement studies. The need of dynamic environmental products to analyze animal movement requires that the increasing number of SRS sensors, the multiple tools and the large quantity of data available become more accessible and easy to use to movement ecologists [307].

4.1. General Observations

Faced with an overabundance of available data, one should gain insight on data quality and the methods, algorithms and applications of using data in animal movement studies. SRS data must often be combined with in-situ measurements, which are sometimes not available, for validation purposes and accurately representation of environmental drivers. SRS has to be considered only as a partial view of the terrain and remain imperfect by definition [308]. Furthermore, the use of SRS products may be limited by the time-span of their availability, their spatial and temporal resolution and coverage, their spectral characteristics (Table 1). The revisit time period of a SRS product (Table 1) does not mean that it will be usable at the same frequency, as the quality of the image may not always be optimal at each acquisition (e.g., cloud cover, limited spatial extent that doesn't cover the desired area, ...).

These limitations often imply a trade-off between spatial and temporal resolutions [309] and/or between spatial resolution and spatial extent coverage [310]. For instance, high and very-high spatial resolution images are not necessarily appropriate for all research questions as they contain large amounts of data, heterogeneity of spectral values and diversity of objects in small spatial extents that can significantly complicate methodology applications [310]. Data pre-processing for a SRS derived application is not only costly in processing time and in expertise but also in financial resources. Naidoo et al. (2012a) estimated that weekly acquisition of very high resolution Quickbird imagery (Table 1) to detect small ephemeral water sources within the frame of their study in relation with buffalo movements would have cost close to USD $9 million [29]. One has to be aware of the computing capacities available, the allowed time and the appropriate algorithm for the completion of SRS analyses [34,311].

4.2. Landcover and Vegetation Characterization

Our review showed that the use of SRS to understand cattle or buffalo movement ecology mainly benefited from open-access products and standard image processing methods. EVI and NDVI are

widely used vegetation indexes to characterize vegetation availability and evolution patterns in these studies [26,29,54,88,312]. However, other spectral indexes such as the Soil Adjusted Vegetation Index (SAVI) (Table 3) that eliminate soil-induced variations in vegetation indexes [143] have not been used at all in existing buffalo and cattle movement studies. The use of such spectral indexes could complement more classic vegetation indexes by overcoming certain associated limitations when characterizing savanna landscapes through SRS approaches (i.e., mixed pixels) [143,313,314].

Few studies listed in this review use high or very high-spatial resolution satellite images to characterize the landcover [54,79,89] comparatively to the studies that use medium or low-spatial resolution satellite images such as MODIS (Table 1) to derive spectral indexes [86,87,135] and Landsat or Spot (Table 1) to characterize landcover [11,70,88,90]. Indeed, high spatial resolution imagery is not necessarily appropriate for all research questions, especially because its limited spatial extent requires the acquisition of several images to cover large areas at a high financial cost [315]. High and very high spatial resolution images contain large amounts of data, heterogeneity of spectral values and diversity of objects that significantly complicate methodology applications such as landcover classification [310]. However, since 2015, open-source Sentinel-2 images (Table 1) bring a spatial resolution and a temporal continuity gain compared to other medium spatial resolution images that could potentially improve spectral indexes or landcover derivation over large areas while maintaining relevance in application for landscape scale analysis.

As the human and livestock populations grow in Africa [2,316], the pressure on protected areas' boundaries increases resulting in the transformation of natural landscapes and the creation of hard edges between protected areas and their surroundings by human infrastructures and activities (e.g., buildings, roads, cleaned land for cultivation, pasture, trees and grasses harvest) [68]. These two factors combined directly impact the movement of buffalo and cattle as they cross the natural park borders to find foraging or water resources. Human infrastructures including fences, human settlements and agricultural areas also represent potential barriers to animal movement. For example, movement rates of buffalos living near fences appear to be low [317] and large migratory movements are limited by fences [146] when they are not damaged by elephants [6]. SRS can play a fundamental role to characterize the human factors (infrastructures, activities) into the buffalo and cattle movement processes. For instance, crops can potentially provide an important resource for both buffalo and cattle during the wet season in southern African savanna even if both species are prevented to enter fields with growing crops (e.g., using different practices such as wildlife deterrent measures and livestock herding). Time series SRS derived vegetation indexes such as EVI or NDVI (Table 3) have been efficiently used as phenology indicators [318,319] combined with landcover classification [320], high-resolution optical and radar sensors [321] for crop and pasture monitoring and space delimitation. Concerning hardly distinguishable objects from space such as fences, human settlements and roads, the increasing availability of very high-resolution (Worldview-2, Pleïades, . . .) satellite images (Table 1) offer a wide range of possibilities to characterize these landscape features via landcover object-based approach classification [23]. These methodologies could certainly be used independently or combined, bringing a wide range of indicators for animal movement and interactions analysis.

4.3. Surface Water Delineation

Several methods such as spectral indexes thresholding (Table 4), image classification, surface water spatial delineation through satellite image textures [184], have been efficiently used independently to map surface water bodies. However, the numerous remote sensing-based water products presented in Table 5 have not been used in the different buffalo and cattle movement reviewed studies. Similarly, water spectral indexes listed in Table 4 and SAR images (Table 1), with the exception of one study that used NDWI derived from Sentinel-2 images in relation with buffalo movements [91], have not been used despite their potential to improve classification algorithms and water detection in savanna environments [177,203,204,207,212]. This may partly result from a lack of knowledge about the

existence and availability of SRS products in the movement ecology community, a major gap that this review aims to fill.

According to our review, the use of SRS offers a potential that remains to be explored regarding the detection of surface water at a landscape scale in savanna environments, as a driver of wild and domestic ungulates movements. Indeed, classification of surface water derived from optical and/or radar medium spatial resolution images (Table 1), could provide spatially delineated surface water areas and water resource seasonal variations at a landscape scale and on a monthly basis (Figure 3B), which constitutes a clear advantage in term of spatial representation over in-situ fixed referenced points.

4.4. Savanna Fire Characterization

SRS plays an important role in determining the spatial extent and timing of fires in savanna environments [244,322]. However,, few of the reviewed studies focusing on buffalo and cattle movements used satellite remote sensing-based fire products (Table 6) and none of them used designed optical images derived fire spectral indexes (Table 7) despite their proven efficiency [323]. Landsat and, increasingly, Sentinel-2 (Table 1) for example, are extensively used for medium spatial resolution fire scar mapping in savanna [250,324] and could provide potential improved results for studies that use lower spatial resolution images [146].

However, mapping fire severity is more challenging than just mapping the occurrence of fire. One major limitation of all optical SRS approaches is the presence of cloud cover that hinders the temporal continuity of the follow-up [325]. For animal movements studies, the severity of a given fire event is more relevant than its frequency and timing alone. To bypass such limitation, SAR images could be used. Philipp and Levick (2020), for example, demonstrated that C-band SAR data can contribute to effectively map fire severity in tropical savanna [325]. Characterizing savanna fire severity in addition of being able to locate fire events could also be useful for measuring more accurately the influence of human land use practices [326] and how it potentially affects animal movements.

4.5. SRS for Precipitation Characterization

According to our review, only the TRMM product (Table 8) have been used for buffalo and cattle movement studies [29,146]. This is probably because most of the satellite-based precipitation products are difficult to apprehend for non-specialists, thus compromising their potential use in animal movement studies. They usually present unconventional output file formats, non-standardised precipitation measurement units and uncommon map projection systems. Therefore, potential users need to access metadata that are most of the time difficult for non-SRS specialist to understand in order to assess satellite-based precipitation products usefulness. The mitigation of this constraint by simplifying the use of satellite-based precipitation products could be greatly beneficial for animal movement studies.

The use of satellite-based precipitation products combined with in-situ precipitation data when available remains paramount for more accurate estimations of precipitation trends at a local scale [272]. Additionally, algorithm performances of satellite-based precipitation products (Table 8) greatly vary depending on location, topography, local climate, and season [273,282,283]. This performance variability needs to be taken into account before choosing a satellite-based precipitation product for a specific application and in accordance with the study area geographical specifications.

4.6. Selection of Suitable SRS Products to Study Buffalo and Cattle Movements in Southern Africa

Choosing a set of SRS tools for the characterisation of environmental drivers influencing the buffalo and cattle movements is firstly driven by the question to be addressed (e.g., habitat selection, landscape scale movement patterns, long-distance migration, . . .), which in turn defines the spatiotemporal scales to be considered [59]. Additional criteria such as the required SRS expertise, computating resources, and cost, may be taken into account too (see Section 4.1). Figure 5 provides an illustration of suitable

SRS products for ecologists to characterize environmental drivers impacting animal movements in southern Africa according to their temporal and spatial resolution scales.

High and very high spatial resolution sensors can be used to provide fine-grain maps of landcover and water surface for habitat occupation and habitat selection studies at local scale. Very high spatial resolution images such as Worldview 2, Pleiades, or Ikonos images can be used to discriminate small objects within the landscape (i.e., fences, human settlements, road networks) and characterize landscape at fine scale (ideal for the study of small animal species with a small home range). However, they are costly and require remote sensing expertise and high computing power.

These fine-scale landcover maps can be combined with precipitation and savanna fires data at coarse spatial resolution but with a high temporal repetitivity for studies that focus on daily animal movements. For instance, precipitation TAMSAT 3.0 (Table 8) product is easily accessible and covers the entire African continent at 4.8 km of spatial resolution with daily, pentadal, decadal, monthly and seasonal temporal resolutions; recent VIIRS active fire images (Table 6) offer improved spatial and temporal resolutions compared to former fire products. These products are easy to use and do not require high computing power.

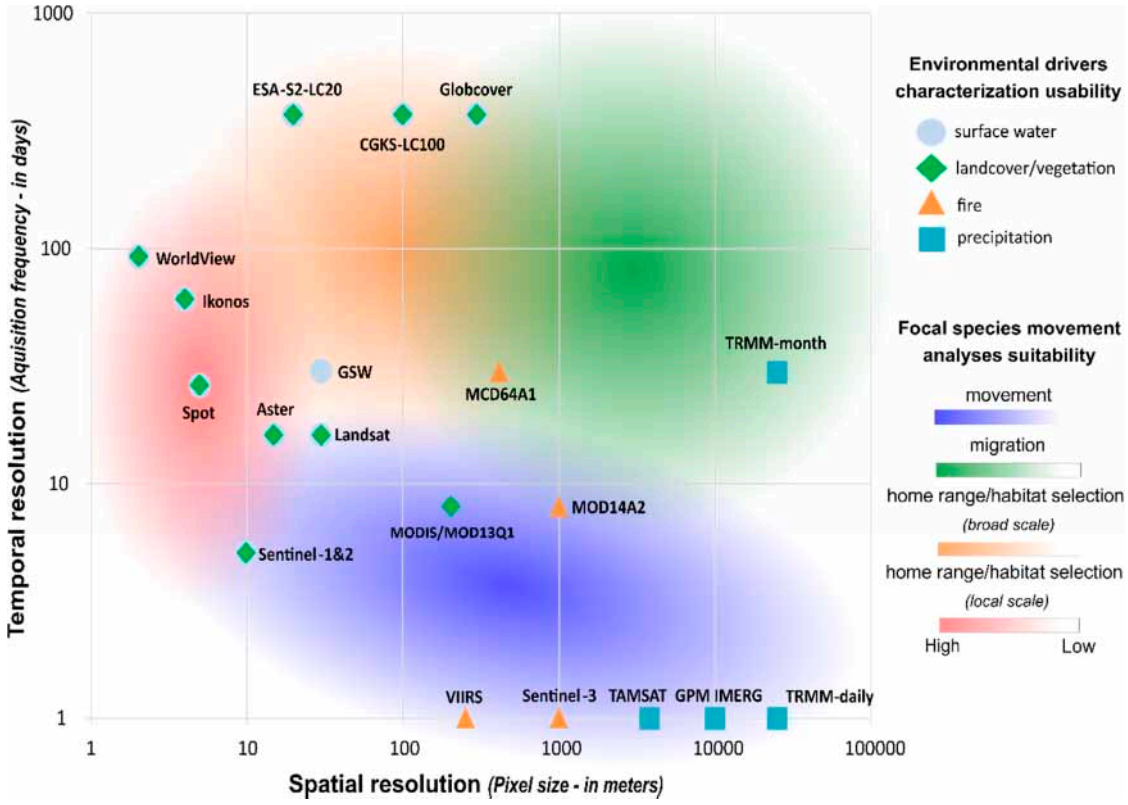

Figure 5. Suitable SRS products for ecologists to characterize environmental drivers impacting animal movements in semi-arid savannas landscapes. These SRS products are represented according to their temporal (ordinate axis) and spatial resolution scales (abscissa axis) and can be used for different type of analyses related to animal movements (movement patterns, home-range and habitat selection at broad and local scales, migration) [59]. We define the "movement" (represented in blue) as the motion initiated by a variety of methods that focal species use to move from one place to another. The "migration" (represented in green) is defined as long distance movements to a different environment involving periodical and cyclical dynamics in space and time. Home range and habitat selection (represented in orange at broad scale and in red at local scale) are considered as areas where focal species regularly move depending on natural resource selections and social interactions and behaviors. Note that the contours of the different analyses categories are blurred to emphazise the fact that there are no clearly established boundaries between these categories.

For studies focusing on animal movements at a coarser spatial and temporal scales, landcover and vegetation (Table 2), fire (Table 6) and water (Table 5) free products can be used for preliminary assessments in areas where in-situ data are difficult to collect or nonexistent. These products are easily accessible online, easy to use for non-SRS specialists, well documented and require little computing power in order to cover large areas. In addition, they can be efficiently combined with higher spatial resolution and custom made SRS products.

5. Conclusions

SRS extends the analytical capacity of ecologists in many fields including animal movement studies [20]. New SRS sensors are continuously launched thus expanding and increasing the potential applications of these tools (Figures 4 and 5). The Committee on Earth Observation Satellites (CEOS) reports that its member agencies are currently operating or planning more than 300 different satellite Earth observation missions by 2030, carrying over 900 different measurement instruments offering different spatial resolutions and spectral capabilities [327]. Medium-resolution Sentinel-1 and Sentinel-2 images (Table 1) are particularly promising in the field of animal movement as they provide continuous open-source data since 2014–2015 at a 10 m spatial resolution with radar and optical sensors. However, given the SRS sensors and applications diversity, it is paramount to determine which SRS product is best suited for a given scale of analyses and how potential inherent limitations can affect the latter.

To facilitate the use of SRS products in ecological movement research studies, a better data accessibility such as the European Spatial Agency Sentinel program, which promotes open data, and training platforms to familiarize users with the utilization and the potentialities of SRS data, are needed. The collaboration of movement ecologists with remote sensing experts within a multi-disciplinary approach could also help to integrate more efficiently remote sensing products in ecological movement research.

Supplementary Materials: The open-source data and developed products presented in Figure 3 are listed below: TAMSAT v3.0 data: the entire archive is available in direct download via batch process at https://www.tamsat.org.uk/data/archive with the script detailed at https://www.tamsat.org.uk/public_data/public_scripts/wget_TAMSATv3.0; The MOD/MYD14A2 (MODIS thermal anomaly product) data are available to download at https://search.earthdata.nasa.gov/search after login—Archived by National Aeronautics and Space Administration, U.S. Government, LP DAAC. https://doi.org/10.5067/MODIS/MOD11A2.006; The MOD/MYD13Q1 (MODIS vegetation product) data are available to download at https://search.earthdata.nasa.gov/search after login—Archived by National Aeronautics and Space Administration, U.S. Government, LP DAAC. https://doi.org/10.5067/MODIS/MOD13Q1.006; The Sentinel-2 images are freely available at https://scihub.copernicus.eu/dhus/#/home after login. The land cover map is available to download at CIRAD depository website: Rumiano, Florent; Miguel, Eve; Valls-Fox, Hugo; Chamaillé-Jammes, Simon; Caron, Alexandre; Tran, Annelise, 2020, "Land cover map, Dete site, Hwangue National Park, Zimbabwe", doi:10.18167/DVN1/BJJZJV, CIRAD Dataverse, V1; The surface water map is available to download at CIRAD depository website: Rumiano, Florent; Miguel, Eve; Valls-Fox, Hugo; Chamaillé-Jammes, Simon; Caron, Alexandre; Tran, Annelise, 2020, "Monthly surface water maps, Hwangue National Park, Zimbabwe, 2018", doi:10.18167/DVN1/KPSYME, CIRAD Dataverse, V1, The buffalo and cattle GPS data access are subject to authors' authorization.

Author Contributions: Conceptualization, F.R. and E.W.; methodology, F.R.; software, F.R.; validation, F.R. and A.T..; formal analysis, F.R.; investigation, F.R.; resources, F.R.; data curation, F.R., E.M., S.C.-J., H.V.-F., D.C., M.D.G.-W. and H.F.; writing—original draft preparation, F.R. and E.W.; writing—review and editing, F.R., E.W., E.M., S.C.-J., H.V.-F., M.D.G.-W., H.F., A.C. and A.T.; visualization, F.R.; supervision, A.C., E.M., A.T.; project administration, A.C., E.M., A.T.; funding acquisition, A.T. and E.M. All authors have read and agreed to the published version of the manuscript.

Funding: This research was funded by I-SITE MUSE (Montpellier Université d'Excellence)—https://muse.edu.umontpellier.fr/en/muse-isite/ through the French National Research Agency (ANR) under the "Investissements d'avenir" program, grant number ANR-16-IDEX-0006.

Acknowledgments: This work is part of a thesis integrated into the TEMPO project (TElédétection et Modélisation sPatiale de la mObilité animale)—https://tempo.cirad.fr/en and is implemented under the framework of the Research Platform "Production and Conservation in Partnership"—www.rp-pcp.org.

Conflicts of Interest: The authors declare no conflict of interest. The funders had no role in the design of the study; in collection, analysis, or interpretation of data; in writing the manuscript; or in the decision to publish the results.

References

1. Cleland, J.; Machiyama, K. The Challenges Posed by Demographic Change in sub-Saharan Africa: A Concise Overview: Challenges Posed by Demographic Change in sub-Saharan Africa. *Popul. Dev. Rev.* **2017**, *43*, 264–286. [CrossRef]
2. Wittemyer, G.; Elsen, P.; Bean, W.T.; Burton, A.C.O.; Brashares, J.S. Accelerated Human Population Growth at Protected Area Edges. *Science* **2008**, *321*, 123–126. [CrossRef] [PubMed]
3. Andersson, J.A.; de Garine-Wichatitsky, M.; Cumming, D.H.M.; Dzingirai, V.; Giller, K.E. *Transfrontier Conservation Areas: People Living on the Edge*, 1st ed.; Routledge: Abingdon, UK, 2017; ISBN 978-1-315-14737-6.
4. De Garine-Wichatitsky, M.; Caron, A.; Kock, R.; Tschopp, R.; Munyeme, M.; Hofmeyr, M.; Michel, A. A review of bovine tuberculosis at the wildlife–livestock–human interface in sub-Saharan Africa. *Epidemiol. Infect.* **2013**, *141*, 1342–1356. [CrossRef] [PubMed]
5. Bengis, R.G.; Kock, R.A.; Fisher, J.R. Infectious animal diseases: The wildlife/livestock interface: -EN- -FR- -ES-. *Rev. Sci. Tech. L'oie* **2002**, *21*, 53–65. [CrossRef]
6. Chigwenhese, L.; Murwira, A.; Zengeya, F.M.; Masocha, M.; de Garine-Wichatitsky, M.; Caron, A. Monitoring African buffalo (*Syncerus caffer*) and cattle (*Bos taurus*) movement across a damaged veterinary control fence at a Southern African wildlife/livestock interface. *Afr. J. Ecol.* **2016**, *54*, 415–423. [CrossRef]
7. Jori, F.; Brahmbhatt, D.; Fosgate, G.T.; Thompson, P.N.; Budke, C.; Ward, M.P.; Ferguson, K.; Gummow, B. A questionnaire-based evaluation of the veterinary cordon fence separating wildlife and livestock along the boundary of the Kruger National Park, South Africa. *Prev. Vet. Med.* **2011**, *100*, 210–220. [CrossRef]
8. Ogutu, J.O.; Owen-Smith, N.; Piepho, H.-P.; Kuloba, B.; Edebe, J. Dynamics of ungulates in relation to climatic and land use changes in an insularized African savanna ecosystem. *Biodivers Conserv.* **2012**, *21*, 1033–1053. [CrossRef]
9. Young, T.P.; Palmer, T.M.; Gadd, M.E. Competition and compensation among cattle, zebras, and elephants in a semi-arid savanna in Laikipia, Kenya. *Biol. Conserv.* **2005**, *122*, 351–359. [CrossRef]
10. Kuiper, T.R.; Loveridge, A.J.; Parker, D.M.; Johnson, P.J.; Hunt, J.E.; Stapelkamp, B.; Sibanda, L.; Macdonald, D.W. Seasonal herding practices influence predation on domestic stock by African lions along a protected area boundary. *Biol. Conserv.* **2015**, *191*, 546–554. [CrossRef]
11. Valls Fox, H. To Drink or Not to Drink? The Influence of Resource Availability on Elephant Foraging and Habitat Selection in a Semi-Arid Savanna. Ph.D. Thesis, Université de Montpellier, Montpellier, France, 2015.
12. Miguel, E.; Grosbois, V.; Caron, A.; Boulinier, T.; Fritz, H.; Cornélis, D.; Foggin, C.; Makaya, P.V.; Tshabalala, P.T.; de Garine-Wichatitsky, M. Contacts and foot and mouth disease transmission from wild to domestic bovines in Africa. *Ecosphere* **2013**, *4*, art51. [CrossRef]
13. Caron, A.; Miguel, E.; Gomo, C.; Makaya, P.; Pfukenyi, D.M.; Foggin, C.; Hove, T.; de Garine-Wichatitsky, M. Relationship between burden of infection in ungulate populations and wildlife/livestock interfaces. *Epidemiol. Infect.* **2013**, *141*, 1522–1535. [CrossRef] [PubMed]
14. Osofsky, S.A.; Cleaveland, S.; Karesh, W.B.; Kock, M.D.; Nyhus, P.J.; College, C. *Conservation and Development Interventions at the Wildlife-Livestock Interface*; IUCN—The World Conservation Union: Gland, Switzerland, 2005; p. 242.
15. Lankester, F.; Davis, A. Pastoralism and wildlife: Historical and current perspectives in the East African rangelands of Kenya and Tanzania. *Rev. Sci. Tech. Oie.* **2016**, *35*, 473–484. [CrossRef] [PubMed]
16. Mascia, M.B.; Pailler, S.; Krithivasan, R.; Roshchanka, V.; Burns, D.; Mlotha, M.J.; Murray, D.R.; Peng, N. Protected area downgrading, downsizing, and degazettement (PADDD) in Africa, Asia, and Latin America and the Caribbean, 1900–2010. *Biol. Conserv.* **2014**, *169*, 355–361. [CrossRef]
17. Ogutu, J.O.; Piepho, H.-P.; Said, M.Y.; Kifugo, S.C. Herbivore Dynamics and Range Contraction in Kajiado County Kenya: Climate and Land Use Changes, Population Pressures, Governance, Policy and Human-wildlife Conflicts. *Toecolj* **2014**, *7*, 9–31. [CrossRef]
18. Mworia, J.K.; Kinyamario, J.I.; Githaiga, J.M. Influence of cultivation, settlements and water sources on wildlife distribution and habitat selection in south-east Kajiado, Kenya. *Environ. Conserv.* **2008**, *35*, 117–124. [CrossRef]
19. Rose, R.A.; Byler, D.; Eastman, J.R.; Fleishman, E.; Geller, G.; Goetz, S.; Guild, L.; Hamilton, H.; Hansen, M.; Headley, R.; et al. Ten ways remote sensing can contribute to conservation. *Conserv. Biol.* **2015**, *29*, 350–359. [CrossRef]

20. Pettorelli, N.; Laurance, W.F.; O'Brien, T.G.; Wegmann, M.; Nagendra, H.; Turner, W. Satellite remote sensing for applied ecologists: Opportunities and challenges. *J. Appl. Ecol.* **2014**, *51*, 839–848. [CrossRef]
21. Zhu, L.; Suomalainen, J.; Liu, J.; Hyyppä, J.; Kaartinen, H.; Haggren, H. A Review: Remote Sensing Sensors. *Multi Purp. Appl. Geospat. Data* **2017**. [CrossRef]
22. Joshi, N.; Baumann, M.; Ehammer, A.; Fensholt, R.; Grogan, K.; Hostert, P.; Jepsen, M.; Kuemmerle, T.; Meyfroidt, P.; Mitchard, E.; et al. A Review of the Application of Optical and Radar Remote Sensing Data Fusion to Land Use Mapping and Monitoring. *Remote Sens.* **2016**, *8*, 70. [CrossRef]
23. Kaszta, Ż.; Van De Kerchove, R.; Ramoelo, A.; Cho, M.; Madonsela, S.; Mathieu, R.; Wolff, E. Seasonal Separation of African Savanna Components Using Worldview-2 Imagery: A Comparison of Pixel- and Object-Based Approaches and Selected Classification Algorithms. *Remote Sens.* **2016**, *8*, 763. [CrossRef]
24. Marghany, M. *Environmental Applications of Remote Sensing*; BoD—Books on Demand: Norderstedt, Germany, 2016; ISBN 978-953-51-2443-6.
25. Pettorelli, N.; Safi, K.; Turner, W. Satellite remote sensing, biodiversity research and conservation of the future. *Philos. Trans. R. Soc. B* **2014**, *369*, 20130190. [CrossRef] [PubMed]
26. Handcock, R.; Swain, D.; Bishop-Hurley, G.; Patison, K.; Wark, T.; Valencia, P.; Corke, P.; O'Neill, C. Monitoring Animal Behaviour and Environmental Interactions Using Wireless Sensor Networks, GPS Collars and Satellite Remote Sensing. *Sensors* **2009**, *9*, 3586–3603. [CrossRef] [PubMed]
27. Hassell, J.M.; Begon, M.; Ward, M.J.; Fèvre, E.M. Urbanization and Disease Emergence: Dynamics at the Wildlife–Livestock–Human Interface. *Trends Ecol. Evol.* **2017**, *32*, 55–67. [CrossRef]
28. Tsalyuk, M.; Kelly, M.; Getz, W.M. Improving the prediction of African savanna vegetation variables using time series of MODIS products. *ISPRS J. Photogramm. Remote Sens.* **2017**, *131*, 77–91. [CrossRef] [PubMed]
29. Naidoo, R.; Preez, P.D.; Stuart-Hill, G.; Chris Weaver, L.; Jago, M.; Wegmann, M. Factors affecting intraspecific variation in home range size of a large African herbivore. *Landsc. Ecol.* **2012**, *27*, 1523–1534. [CrossRef]
30. Mitchard, E.T.A.; Flintrop, C.M. Woody encroachment and forest degradation in sub-Saharan Africa's woodlands and savannas 1982–2006. *Philos. Trans. R. Soc. B Biol. Sci.* **2013**, *368*, 20120406. [CrossRef] [PubMed]
31. Mathieu, R.; Wessels, K.; Asner, G.; Knapp, D.; van Aardt, J.; Main, R.; Cho, M.; Erasmus, B.; Smit, I. Tree cover, tree height and bare soil cover differences along a land use degradation gradient in semi-arid savannas, South Africa. In Proceedings of the 2009 IEEE International Geoscience and Remote Sensing Symposium, Cape Town, South Africa, 12–17 July 2009; Volume 2, pp. II-194–II-197.
32. Forkuor, G.; Benewinde Zoungrana, J.-B.; Dimobe, K.; Ouattara, B.; Vadrevu, K.P.; Tondoh, J.E. Above-ground biomass mapping in West African dryland forest using Sentinel-1 and 2 datasets—A case study. *Remote Sens. Environ.* **2020**, *236*, 111496. [CrossRef]
33. Yang, J.; Prince, S.D. Remote sensing of savanna vegetation changes in Eastern Zambia 1972–1989. *Int. J. Remote Sens.* **2000**, *21*, 301–322. [CrossRef]
34. Chuvieco, E. *Fundamentals of Satellite Remote Sensing: An Environmental Approach*, 2nd ed.; CRC Press: Boca Raton, FL, USA, 2016; ISBN 978-1-4987-2807-2.
35. Eisfelder, C.; Kuenzer, C.; Dech, S. Derivation of biomass information for semi-arid areas using remote-sensing data. *Int. J. Remote Sens.* **2012**, *33*, 2937–2984. [CrossRef]
36. Pruvot, M.; Musiani, M.; Boyce, M.S.; Kutz, S.; Orsel, K. Integrating livestock management and telemetry data to assess disease transmission risk between wildlife and livestock. *Prev. Vet. Med.* **2020**, *174*, 104846. [CrossRef]
37. Miguel, E.; Grosbois, V.; Fritz, H.; Caron, A.; de Garine-Wichatitsky, M.; Nicod, F.; Loveridge, A.J.; Stapelkamp, B.; Macdonald, D.W.; Valeix, M. Drivers of foot-and-mouth disease in cattle at wild/domestic interface: Insights from farmers, buffalo and lions. *Divers. Distrib.* **2017**, *23*, 1018–1030. [CrossRef] [PubMed]
38. Hebblewhite, M.; Merrill, E.; McDermid, G. A Multi-Scale Test of the Forage Maturation Hypothesis in a Partially Migratory Ungulate Population. *Ecol. Monogr.* **2008**, *78*, 141–166. [CrossRef]
39. Williams, P.H.; Burgess, N.D.; Rahbek, C. Flagship species, ecological complementarity and conserving the diversity of mammals and birds in sub-Saharan Africa. *Anim. Conserv.* **2000**, *3*, 249–260. [CrossRef]
40. Lindsey, P.A.; Roulet, P.A.; Romañach, S.S. Economic and conservation significance of the trophy hunting industry in sub-Saharan Africa. *Biol. Conserv.* **2007**, *134*, 455–469. [CrossRef]
41. Van der Merwe, P.; Saayman, M. Game farms as sustainable ecotourist attractions. *Koedoe* **2005**, *48*, 1–10. [CrossRef]

42. Barnett, R. *Food for Thought: The Utilization of Wild Meat in Eastern and Southern Africa*; TRAFFIC East-Southern Africa: Nairobi, Kenya, 2000; ISBN 978-9966-9698-0-4.
43. Eby, S.; Burkepile, D.E.; Fynn, R.W.S.; Burns, C.E.; Govender, N.; Hagenah, N.; Koerner, S.E.; Matchett, K.J.; Thompson, D.I.; Wilcox, K.R.; et al. Loss of a large grazer impacts savanna grassland plant communities similarly in North America and South Africa. *Oecologia* **2014**, *175*, 293–303. [CrossRef]
44. Estes, R.D. *The Behavior Guide to African Mammals: Including Hoofed Mammals, Carnivores, Primates*; The University of California Press: Berkeley, CA, USA, 2012.
45. Munag'andu, H.M.; Siamudaala, V.M.; Nambota, A.; Bwalya, J.M.; Munyeme, M.; Mweene, A.S.; Takada, A.; Kida, H. Disease constraints for utilization of the African buffalo (*Syncerus caffer*) on game ranches in Zambia. *Jpn. J. Vet. Sci.* **2006**, *11*, 3–13.
46. Prins, H. *Ecology and Behaviour of the African Buffalo: Social Inequality and Decision Making*; Springer Science & Business Media: Berlin, Germany, 1996; ISBN 978-0-412-72520-3.
47. Ndengu, M.; De Garine-Wichatitsky, M.; Pfukenyi, D.M.; Tivapasi, M.; Mukamuri, B.; Matope, G. Assessment of community awareness and risk perceptions of zoonotic causes of abortion in cattle at three selected livestock–wildlife interface areas of Zimbabwe. *Epidemiol. Infect.* **2017**, *145*, 1304–1319. [CrossRef]
48. Baudron, F.; Andersson, J.A.; Corbeels, M.; Giller, K.E. Failing to Yield? Ploughs, Conservation Agriculture and the Problem of Agricultural Intensification: An Example from the Zambezi Valley, Zimbabwe. *J. Dev. Stud.* **2012**, *48*, 393–412. [CrossRef]
49. Mapiye, C.; Chimonyo, M.; Dzama, K. Seasonal dynamics, production potential and efficiency of cattle in the sweet and sour communal rangelands in South Africa. *J. Arid. Environ.* **2009**. [CrossRef]
50. Hoffmann, I. Spatial distribution of cattle herds as a response to naturaland social environments: A case study from the Zamfara Reserve, Northwestern Nigeria. *Nomadic Peoples* **2002**, *6*, 4–21. [CrossRef]
51. Augustine, D.J. Response of native ungulates to drought in semi-arid Kenyan rangeland: Ungulate response to drought. *Afr. J. Ecol.* **2010**, *48*, 1009–1020. [CrossRef]
52. Odadi, W.O.; Karachi, M.K.; Abdulrazak, S.A.; Young, T.P. African Wild Ungulates Compete with or Facilitate Cattle Depending on Season. *Science* **2011**, *333*, 1753–1755. [CrossRef] [PubMed]
53. Kaszta, Ż.; Cushman, S.A.; Sillero-Zubiri, C.; Wolff, E.; Marino, J. Where buffalo and cattle meet: Modelling interspecific contact risk using cumulative resistant kernels. *Ecography* **2018**, *41*, 1616–1626. [CrossRef]
54. Zengeya, F.M.; Murwira, A.; Caron, A.; Cornélis, D.; Gandiwa, P.; de Garine-Wichatitsky, M. Spatial overlap between sympatric wild and domestic herbivores links to resource gradients. *Remote Sens. Appl. Soc. Environ.* **2015**, *2*, 56–65. [CrossRef]
55. Dougherty, E.R.; Seidel, D.P.; Carlson, C.J.; Getz, W.M. Using Movement Data to Estimate Contact Rates in a Simulated Environmentally-Transmitted Disease System. *Ecology* **2018**. [CrossRef]
56. Van Schalkwyk, O.L.; Knobel, D.L.; Clercq, E.M.D.; Pus, C.D.; Hendrickx, G.; Van den Bossche, P.V. Description of Events Where African Buffaloes (Syncerus caffer) Strayed from the Endemic Foot-and-Mouth Disease Zone in South Africa, 1998–2008. *Transbound. Emerg. Dis.* **2016**, *63*, 333–347. [CrossRef]
57. Jori, F.; Vosloo, W.; Du Plessis, B.J.A.; Brahmbhatt, D.; Gummow, B.; Thomson, G.R. A qualitative risk assessment of factors contributing to foot and mouth disease outbreaks in cattle along the western boundary of the Kruger National Park. *Rev. Sci. Tech. Oie.* **2009**, *28*, 917–931. [CrossRef]
58. Kock, R.A. The Wildlife Domestic Animal Disease Interface—Should Africa adopt a hard or soft edge? *Trans. R. Soc. S. Afr.* **2004**, *59*, 10–14. [CrossRef]
59. Neumann, W.; Martinuzzi, S.; Estes, A.B.; Pidgeon, A.M.; Dettki, H.; Ericsson, G.; Radeloff, V.C. Opportunities for the application of advanced remotely-sensed data in ecological studies of terrestrial animal movement. *Mov. Ecol.* **2015**, *3*, 8. [CrossRef]
60. Grant, M.J.; Booth, A. A typology of reviews: An analysis of 14 review types and associated methodologies. *Health Inf. Libr. J.* **2009**, *26*, 91–108. [CrossRef]
61. Drusch, M.; Del Bello, U.; Carlier, S.; Colin, O.; Fernandez, V.; Gascon, F.; Hoersch, B.; Isola, C.; Laberinti, P.; Martimort, P.; et al. Sentinel-2: ESA's Optical High-Resolution Mission for GMES Operational Services. *Remote Sens. Environ.* **2012**, *120*, 25–36. [CrossRef]
62. Tarnavsky, E.; Grimes, D.; Maidment, R.; Black, E.; Allan, R.P.; Stringer, M.; Chadwick, R.; Kayitakire, F. Extension of the TAMSAT Satellite-Based Rainfall Monitoring over Africa and from 1983 to Present. *J. Appl. Meteor. Clim.* **2014**, *53*, 2805–2822. [CrossRef]

63. Maidment, R.I.; Grimes, D.; Allan, R.P.; Tarnavsky, E.; Stringer, M.; Hewison, T.; Roebeling, R.; Black, E. The 30 year TAMSAT African Rainfall Climatology And Time series (TARCAT) data set: 30-YEAR AFRICAN RAINFALL DATASET. *J. Geophys. Res. Atmos.* **2014**, *119*, 10,619–10,644. [CrossRef]
64. Doherty, T.S.; Driscoll, D.A. Coupling movement and landscape ecology for animal conservation in production landscapes. *Proc. R. Soc. B Biol. Sci.* **2018**, *285*, 20172272. [CrossRef]
65. Tyrrell, P.; Russell, S.; Western, D. Seasonal movements of wildlife and livestock in a heterogenous pastoral landscape: Implications for coexistence and community based conservation. *Glob. Ecol. Conserv.* **2017**, *12*, 59–72. [CrossRef]
66. Owen-Smith, N.; Mills, M.G.L. Predator–prey size relationships in an African large-mammal food web. *J. Anim. Ecol.* **2008**, *77*, 173–183. [CrossRef]
67. Odadi, W.O.; Young, T.P.; Okeyo-Owuor, J.B. Effects of Wildlife on Cattle Diets in Laikipia Rangeland, Kenya. *Rangel. Ecol. Manag.* **2007**, *60*, 179–185. [CrossRef]
68. Hibert, F.; Calenge, C.; Fritz, H.; Maillard, D.; Bouché, P.; Ipavec, A.; Convers, A.; Ombredane, D.; de Visscher, M.-N. Spatial avoidance of invading pastoral cattle by wild ungulates: Insights from using point process statistics. *Biodivers Conserv.* **2010**, *19*, 2003–2024. [CrossRef]
69. Hofmann, R.R. Evolutionary steps of ecophysiological adaptation and diversification of ruminants: A comparative view of their digestive system. *Oecologia* **1989**, *78*, 443–457. [CrossRef]
70. Tambling, C.J.; Druce, D.J.; Hayward, M.W.; Castley, J.G.; Adendorff, J.; Kerley, G.I.H. Spatial and temporal changes in group dynamics and range use enable anti-predator responses in African buffalo. *Ecology* **2012**, *93*, 1297–1304. [CrossRef] [PubMed]
71. Furstenburg, D. *African Buffalo Syncerus Caffer*; Geo Wild Consult (Pty) Ltd.: Gauteng, South Africa, 2010; p. 18.
72. Tshabalala, T.; Dube, S.; Lent, P.C. Seasonal variation in forages utilized by the African buffalo (*Syncerus caffer*) in the succulent thicket of South Africa: Seasonal variation in buffalo diet. *Afr. J. Ecol.* **2009**, *48*, 438–445. [CrossRef]
73. Macandza, V.A.; Owen-Smith, N.; Cross, P.C. Forage selection by African buffalo in the late dry season in two landscapes. *Afr. J. Wildl. Res.* **2004**, *34*, 9.
74. Hendricks, H.H.; Clark, B.; Bond, W.J.; Midgley, J.J.; Novellie, P.A. Movement response patterns of livestock to rainfall variability in the Richtersveld National Park. *Afr. J. Range Forage Sci.* **2005**, *22*, 117–125. [CrossRef]
75. Kartzinel, T.R.; Chen, P.A.; Coverdale, T.C.; Erickson, D.L.; Kress, W.J.; Kuzmina, M.L.; Rubenstein, D.I.; Wang, W.; Pringle, R.M. DNA metabarcoding illuminates dietary niche partitioning by African large herbivores. *Proc. Natl. Acad. Sci. USA* **2015**, *112*, 8019–8024. [CrossRef] [PubMed]
76. Prins, H.H.T. Condition Changes and Choice of Social Environment in African Buffalo Bulls. *Behaviour* **1989**, *108*, 297–323. [CrossRef]
77. Stark, M. Daily Movement, Grazing Activity and Diet of Savanna Buffalo, Syncerus-Caffer-Brachyceros, in Benoue-National-Park, Cameroon. *Afr. J. Ecol.* **1986**, *24*, 255–262. [CrossRef]
78. Sianga, K.; Fynn, R.W.S.; Bonyongo, M.C. Seasonal habitat selection by African buffalo *Syncerus caffer* in the Savuti–Mababe–Linyanti ecosystem of northern Botswana. *Koedoe* **2017**, 59. [CrossRef]
79. Kaszta, Ż.; Marino, J.; Wolff, E. Fine-scale spatial and seasonal rangeland use by cattle in a foot-and-mouth disease control zones. *Agric. Ecosyst. Environ.* **2017**, *239*, 161–172. [CrossRef]
80. Hansen, M.C.; Potapov, P.V.; Moore, R.; Hancher, M.; Turubanova, S.A.; Tyukavina, A.; Thau, D.; Stehman, S.V.; Goetz, S.J.; Loveland, T.R.; et al. High-Resolution Global Maps of 21st-Century Forest Cover Change. *Science* **2013**, *342*, 850–853. [CrossRef]
81. Mayaux, P.; Bartholomé, E.; Fritz, S.; Belward, A. A new land-cover map of Africa for the year 2000: New land-cover map of Africa. *J. Biogeogr.* **2004**, *31*, 861–877. [CrossRef]
82. Friedl, M.A.; McIver, D.K.; Hodges, J.C.F.; Zhang, X.Y.; Muchoney, D.; Strahler, A.H.; Woodcock, C.E.; Gopal, S.; Schneider, A.; Cooper, A.; et al. Global land cover mapping from MODIS: Algorithms and early results. *Remote Sens. Environ.* **2002**, *83*, 287–302. [CrossRef]
83. Loveland, T.R.; Reed, B.C.; Brown, J.F.; Ohlen, D.O.; Zhu, Z.; Yang, L.; Merchant, J.W. Development of a global land cover characteristics database and IGBP DISCover from 1 km AVHRR data. *Int. J. Remote Sens.* **2000**, *21*, 1303–1330. [CrossRef]
84. Townshend, J.; Justice, C.; Li, W.; Gurney, C.; McManus, J. Global land cover classification by remote sensing: Present capabilities and future possibilities. *Remote Sens. Environ.* **1991**, *35*, 243–255. [CrossRef]

85. Corbane, C.; Lang, S.; Pipkins, K.; Alleaume, S.; Deshayes, M.; García Millán, V.E.; Strasser, T.; Vanden Borre, J.; Toon, S.; Michael, F. Remote sensing for mapping natural habitats and their conservation status—New opportunities and challenges. *Int. J. Appl. Earth Obs. Geoinf.* **2015**, *37*, 7–16. [CrossRef]
86. Pettorelli, N.; Bro-Jørgensen, J.; Durant, S.M.; Blackburn, T.; Carbone, C. Energy Availability and Density Estimates in African Ungulates. *Am. Nat.* **2009**, *173*, 698–704. [CrossRef]
87. Bro-Jørgensen, J.; Brown, M.E.; Pettorelli, N. Using the satellite-derived normalized difference vegetation index (NDVI) to explain ranging patterns in a lek-breeding antelope: The importance of scale. *Oecologia* **2008**, *158*, 177–182. [CrossRef]
88. Cornélis, D.; Benhamou, S.; Janeau, G.; Morellet, N.; Ouedraogo, M.; de Visscher, M.-N. Spatiotemporal dynamics of forage and water resources shape space use of West African savanna buffaloes. *J. Mammal.* **2011**, *92*, 1287–1297. [CrossRef]
89. Zengeya, F.M.; Murwira, A.; Garine-Wichatitsky, M.D. Seasonal habitat selection and space use by a semi-free range herbivore in a heterogeneous savanna landscape. *Austral Ecol.* **2014**, *39*, 722–731. [CrossRef]
90. Valls-Fox, H.; Chamaillé-Jammes, S.; de Garine-Wichatitsky, M.; Perrotton, A.; Courbin, N.; Miguel, E.; Guerbois, C.; Caron, A.; Loveridge, A.; Stapelkamp, B.; et al. Water and cattle shape habitat selection by wild herbivores at the edge of a protected area. *Anim. Conserv.* **2018**, *21*, 365–375. [CrossRef]
91. Naidoo, R.; Brennan, A.; Shapiro, A.C.; Beytell, P.; Aschenborn, O.; Preez, P.D.; Kilian, J.W.; Stuart-Hill, G.; Taylor, R.D. Mapping and assessing the impact of small-scale ephemeral water sources on wildlife in an African seasonal savannah. *Ecol. Appl.* **2020**, e02203. [CrossRef]
92. Zengeya, F.; Murwira, A.; de Garine-Wichatitsky, M. An IKONOS-based comparison of methods to estimate cattle home ranges in a semi-arid landscape of southern Africa. *Int. J. Remote Sens.* **2011**, *32*, 7805–7826. [CrossRef]
93. Rodriguez-Galiano, V.F.; Ghimire, B.; Rogan, J.; Chica-Olmo, M.; Rigol-Sanchez, J.P. An assessment of the effectiveness of a random forest classifier for land-cover classification. *ISPRS J. Photogramm. Remote Sens.* **2012**, *67*, 93–104. [CrossRef]
94. Breiman, L. Random forests. *Mach. Learn.* **2001**, *45*, 5–32. [CrossRef]
95. Ghimire, B.; Rogan, J.; Miller, J. Contextual land-cover classification: Incorporating spatial dependence in land-cover classification models using random forests and the Getis statistic. *Remote Sens. Lett.* **2010**, *1*, 45–54. [CrossRef]
96. Chan, J.C.-W.; Paelinckx, D. Evaluation of Random Forest and Adaboost tree-based ensemble classification and spectral band selection for ecotope mapping using airborne hyperspectral imagery. *Remote Sens. Environ.* **2008**, *112*, 2999–3011. [CrossRef]
97. Du, P.; Samat, A.; Waske, B.; Liu, S.; Li, Z. Random Forest and Rotation Forest for fully polarized SAR image classification using polarimetric and spatial features. *ISPRS J. Photogramm. Remote Sens.* **2015**, *105*, 38–53. [CrossRef]
98. Gislason, P.O.; Benediktsson, J.A.; Sveinsson, J.R. Random Forests for land cover classification. *Pattern Recognit. Lett.* **2006**, *27*, 294–300. [CrossRef]
99. Duda, T.; Canty, M. Unsupervised classification of satellite imagery: Choosing a good algorithm. *Int. J. Remote Sens.* **2002**, *23*, 2193–2212. [CrossRef]
100. Blaschke, T.; Hay, G.J.; Kelly, M.; Lang, S.; Hofmann, P.; Addink, E.; Queiroz Feitosa, R.; van der Meer, F.; van der Werff, H.; van Coillie, F.; et al. Geographic Object-Based Image Analysis—Towards a new paradigm. *ISPRS J. Photogramm. Remote Sens.* **2014**, *87*, 180–191. [CrossRef]
101. Xu, Y.; Yu, L.; Feng, D.; Peng, D.; Li, C.; Huang, X.; Lu, H.; Gong, P. Comparisons of three recent moderate resolution African land cover datasets: CGLS-LC100, ESA-S2-LC20, and FROM-GLC-Africa30. *Int. J. Remote Sens.* **2019**, *40*, 6185–6202. [CrossRef]
102. Arraut, E.M.; Loveridge, A.J.; Chamaillé-Jammes, S.; Valls-Fox, H.; Macdonald, D.W. The 2013–2014 vegetation structure map of Hwange National Park, Zimbabwe, produced using free satellite images and software. *Koedoe Afr. Prot. Area Conserv. Sci.* **2018**, 60. [CrossRef]
103. Liu, B.; Chen, J.; Chen, J.; Zhang, W. Land Cover Change Detection Using Multiple Shape Parameters of Spectral and NDVI Curves. *Remote Sens.* **2018**, *10*, 1251. [CrossRef]
104. Münch, Z.; Gibson, L.; Palmer, A. Monitoring Effects of Land Cover Change on Biophysical Drivers in Rangelands Using Albedo. *Land* **2019**, *8*, 33. [CrossRef]

105. Gómez, C.; White, J.C.; Wulder, M.A. Optical remotely sensed time series data for land cover classification: A review. *ISPRS J. Photogramm. Remote Sens.* **2016**, *116*, 55–72. [CrossRef]
106. Balzter, H.; Cole, B.; Thiel, C.; Schmullius, C. Mapping CORINE Land Cover from Sentinel-1A SAR and SRTM Digital Elevation Model Data using Random Forests. *Remote Sens.* **2015**, *7*, 14876–14898. [CrossRef]
107. Longepe, N.; Rakwatin, P.; Isoguchi, O.; Shimada, M.; Uryu, Y.; Yulianto, K. Assessment of ALOS PALSAR 50 m Orthorectified FBD Data for Regional Land Cover Classification by Support Vector Machines. *IEEE Trans. Geosci. Remote Sens.* **2011**, *49*, 2135–2150. [CrossRef]
108. Abdikan, S.; Sanli, F.B.; Ustuner, M.; Calò, F. Land Cover Mapping Using Sentinel-1 SAR Data. *Int. Arch. Photogramm. Remote Sens. Spat. Inf. Sci.* **2016**, *XLI-B7*, 757–761. [CrossRef]
109. Reiche, J.; Verhoeven, R.; Verbesselt, J.; Hamunyela, E.; Wielaard, N.; Herold, M. Characterizing Tropical Forest Cover Loss Using Dense Sentinel-1 Data and Active Fire Alerts. *Remote Sens.* **2018**, *10*, 777. [CrossRef]
110. Bouvet, A.; Mermoz, S.; Le Toan, T.; Villard, L.; Mathieu, R.; Naidoo, L.; Asner, G.P. An above-ground biomass map of African savannahs and woodlands at 25m resolution derived from ALOS PALSAR. *Remote Sens. Environ.* **2018**, *206*, 156–173. [CrossRef]
111. De Alban, J.D.T.; Connette, G.M.; Oswald, P.; Webb, E.L. Combined Landsat and L-Band SAR Data Improves Land Cover Classification and Change Detection in Dynamic Tropical Landscapes. *Remote Sens.* **2018**, *10*, 306. [CrossRef]
112. Mercier, A.; Betbeder, J.; Rumiano, F.; Gond, V.; Bourgoin, C.; Cornu, G.; Blanc, L.; Baudry, J.; Huber-Moy, L. Evaluation of the joint use of Sentinel-1 & 2 time series for land cover classification of large areas: From temperate to tropical landscapes. *Remoste Sens.* **2018**, *11*, 979. [CrossRef]
113. Reiche, J.; Lucas, R.; Mitchell, A.L.; Verbesselt, J.; Hoekman, D.H.; Haarpaintner, J.; Kellndorfer, J.M.; Rosenqvist, A.; Lehmann, E.A.; Woodcock, C.E.; et al. Combining satellite data for better tropical forest monitoring. *Nat. Clim. Chang.* **2016**, *6*, 120–122. [CrossRef]
114. Li, W.; MacBean, N.; Ciais, P.; Defourny, P.; Lamarche, C.; Bontemps, S.; Houghton, R.A.; Peng, S. Gross and net land cover changes in the main plant functional types derived from the annual ESA CCI land cover maps (1992–2015). *Earth Syst. Sci. Data* **2018**, *10*, 219–234. [CrossRef]
115. Friedl, M.A.; Sulla-Menashe, D.; Tan, B.; Schneider, A.; Ramankutty, N.; Sibley, A.; Huang, X. MODIS Collection 5 global land cover: Algorithm refinements and characterization of new datasets. *Remote Sens. Environ.* **2010**, *114*, 168–182. [CrossRef]
116. Chen, J.; Chen, J.; Liao, A.; Cao, X.; Chen, L.; Chen, X.; He, C.; Han, G.; Peng, S.; Lu, M.; et al. Global land cover mapping at 30m resolution: A POK-based operational approach. *Isprs J. Photogramm. Remote Sens.* **2015**, *103*, 7–27. [CrossRef]
117. Bartholomé, E.; Belward, A.S. GLC2000: A new approach to global land cover mapping from Earth observation data. *Int. J. Remote Sens.* **2005**, *26*, 1959–1977. [CrossRef]
118. Arino, O.; Ramos Perez, J.J.; Kalogirou, V.; Bontemps, S.; Defourny, P.; Van Bogaert, E. *Global Land Cover Map for 2009 (GlobCover 2009)*; © European Space Agency (ESA) & Université catholique de Louvain (UCL), PANGAEA: Paris, France; Louvain, Belgium, 2012. [CrossRef]
119. Tateishi, R.; Uriyangqai, B.; Al-Bilbisi, H.; Ghar, M.A.; Tsend-Ayush, J.; Kobayashi, T.; Kasimu, A.; Hoan, N.T.; Shalaby, A.; Alsaaideh, B.; et al. Production of global land cover data—GLCNMO. *Int. J. Digit. Earth* **2011**, *4*, 22–49. [CrossRef]
120. Latham, J.S.; Cumani, R. Global Land Cover SHARE (GLC-SHARE) Database Beta-Release Version 1.0. 2014. Available online: http://www.fao.org/uploads/media/glc-share-doc.pdf (accessed on 3 July 2020).
121. Wang, J.; Zhao, Y.; Li, C.; Yu, L.; Liu, D.; Gong, P. Mapping global land cover in 2001 and 2010 with spatial-temporal consistency at 250 m resolution. *ISPRS J. Photogramm. Remote Sens.* **2015**, *103*, 38–47. [CrossRef]
122. Gong, P.; Wang, J.; Yu, L.; Zhao, Y.; Zhao, Y.; Liang, L.; Niu, Z.; Huang, X.; Fu, H.; Liu, S.; et al. Finer resolution observation and monitoring of global land cover: First mapping results with Landsat TM and ETM+ data. *Int. J. Remote Sens.* **2013**, *34*, 2607–2654. [CrossRef]
123. Sexton, J.O.; Song, X.-P.; Feng, M.; Noojipady, P.; Anand, A.; Huang, C.; Kim, D.-H.; Collins, K.M.; Channan, S.; DiMiceli, C.; et al. Global, 30-m resolution continuous fields of tree cover: Landsat-based rescaling of MODIS vegetation continuous fields with lidar-based estimates of error. *Int. J. Digit. Earth* **2013**, *6*, 427–448. [CrossRef]

124. Buchhorn, M.; Bertels, L.; Smets, B.; Lesiv, M.; Wur, N.E.T. Copernicus Global Land Operations "Vegetation and Energy". 2017. Available online: https://land.copernicus.eu/global/sites/cgls.vito.be/files/products/CGLOPS1_PUM_LC100m-V1_I1.00.pdf (accessed on 3 July 2020).
125. Lesiv, M.; Fritz, S.; McCallum, I.; Tsendbazar, N.; Herold, M.; Pekel, J.-F.; Buchhorn, M.; Smets, B.; Van De Kerchove, R. Evaluation of ESA CCI Prototype Land Cover Map at 20 m. 2017. Available online: http://pure.iiasa.ac.at/id/eprint/14979/ (accessed on 3 July 2020).
126. Jianya, G.; Haigang, S.; Guorui, M.; Qiming, Z. A Review of multi-temporal remote sensing data change detection algorithms. *Remote Sens.* **2008**, *5*, 7.
127. Vanderpost, C.; Ringrose, S.; Matheson, W.; Arntzen, J. Satellite based long-term assessment of rangeland condition in semi-arid areas: An example from Botswana. *J. Arid Environ.* **2011**, *75*, 383–389. [CrossRef]
128. Kindu, M.; Schneider, T.; Teketay, D.; Knoke, T. Land Use/Land Cover Change Analysis Using Object-Based Classification Approach in Munessa-Shashemene Landscape of the Ethiopian Highlands. *Remote Sens.* **2013**, *5*, 2411–2435. [CrossRef]
129. Kerr, J.T.; Ostrovsky, M. From space to species: Ecological applications for remote sensing. *Trends Ecol. Evol.* **2003**, *18*, 299–305. [CrossRef]
130. Turner, W.; Spector, S.; Gardiner, N.; Fladeland, M.; Sterling, E.; Steininger, M. Remote sensing for biodiversity science and conservation. *Trends Ecol. Evol.* **2003**, *18*, 306–314. [CrossRef]
131. Pettorelli, N.; Vik, J.O.; Mysterud, A.; Gaillard, J.-M.; Tucker, C.J.; Stenseth, N.C. Using the satellite-derived NDVI to assess ecological responses to environmental change. *Trends Ecol. Evol.* **2005**, *20*, 503–510. [CrossRef]
132. Wang, Q.; Adiku, S.; Tenhunen, J.; Granier, A. On the relationship of NDVI with leaf area index in a deciduous forest site. *Remote Sens. Environ.* **2005**, *94*, 244–255. [CrossRef]
133. Buermann, W. Analysis of a multiyear global vegetation leaf area index data set. *J. Geophys. Res.* **2002**, *107*, 4646. [CrossRef]
134. Myneni, R.B.; Hall, F.G.; Sellers, P.J.; Marshak, A.L. The interpretation of spectral vegetation indexes. *IEEE Trans. Geosci. Remote Sens.* **1995**, *33*, 481–486. [CrossRef]
135. Ryan, S.J.; Cross, P.C.; Winnie, J.; Hay, C.; Bowers, J.; Getz, W.M. The utility of normalized difference vegetation index for predicting African buffalo forage quality. *J. Wildl. Manag.* **2012**, *76*, 1499–1508. [CrossRef]
136. Hamel, S.; Garel, M.; Festa-Bianchet, M.; Gaillard, J.-M.; Côté, S.D. Spring Normalized Difference Vegetation Index (NDVI) predicts annual variation in timing of peak faecal crude protein in mountain ungulates. *J. Appl. Ecol.* **2009**, *46*, 582–589. [CrossRef]
137. Pettorelli, N.; Pelletier, F.; von Hardenberg, A.; Festa-Bianchet, M.; Côté, S.D. Early Onset of Vegetation Growth Vs. Rapid Green-up: Impacts on Juvenile Mountain Ungulates. *Ecology* **2007**, *88*, 381–390. [CrossRef] [PubMed]
138. MØller, A.P.; Merilä, J. Analysis and Interpretation of Long-Term Studies Investigating Responses to Climate Change. In *Advances in Ecological Research*; Birds and Climate Change; Academic Press: Cambridge, MA, USA, 2004; Volume 35, pp. 111–130.
139. Andersen, R.; Herfindel, I.; Sæther, B.-E.; Linnell, J.D.C.; Oddén, J.; Liberg, O. When range expansion rate is faster in marginal habitats. *Oikos* **2004**, *107*, 210–214. [CrossRef]
140. Guan, K.; Wood, E.F.; Medvigy, D.; Kimball, J.; Pan, M.; Caylor, K.K.; Sheffield, J.; Xu, X.; Jones, M.O. Terrestrial hydrological controls on land surface phenology of African savannas and woodlands: Hydrology controls on African phenology. *J. Geophys. Res. Biogeosci.* **2014**, *119*, 1652–1669. [CrossRef]
141. Archibald, S.; Hempson, G.P. Competing consumers: Contrasting the patterns and impacts of fire and mammalian herbivory in Africa. *Phil. Trans. R. Soc. B* **2016**, *371*, 20150309. [CrossRef]
142. Pinty, B.; Verstraete, M.M. GEMI: A non-linear index to monitor global vegetation from satellites. *Vegetation* **1992**, *101*, 15–20. [CrossRef]
143. Huete, A.R. A soil-adjusted vegetation index (SAVI). *Remote Sens. Environ.* **1988**, *25*, 295–309. [CrossRef]
144. Tsalyuk, M.; Kilian, W.; Reineking, B.; Getz, W.M. Temporal variation in resource selection of African elephants follows long-term variability in resource availability. *Ecol. Monogr.* **2019**, *89*, e01348. [CrossRef]
145. Boone, R.B.; Thirgood, S.J.; Hopcraft, J.G.C. Serengeti Wildebeest Migratory Patterns Modeled from Rainfall and New Vegetation Growth. Available online: https://esajournals.onlinelibrary.wiley.com/doi/abs/10.1890/00129658%282006%2987%5B1987%3ASWMPMF%5D2.0.CO%3B2 (accessed on 13 August 2019).
146. Naidoo, R.; Du Preez, P.; Stuart-Hill, G.; Jago, M.; Wegmann, M. Home on the Range: Factors Explaining Partial Migration of African Buffalo in a Tropical Environment. *PLoS ONE* **2012**, *7*, e36527. [CrossRef]

147. Sitters, J.; Heitkönig, I.M.A.; Holmgren, M.; Ojwang', G.S.O. Herded cattle and wild grazers partition water but share forage resources during dry years in East African savannas. *Biol. Conserv.* **2009**, *142*, 738–750. [CrossRef]
148. Huete, A.R.; Liu, H.Q.; Batchily, K.; Leeuwen, W. van A comparison of vegetation indices over a global set of TM images for EOS-MODIS. *Remote Sens. Environ.* **1997**, *59*, 440–451. [CrossRef]
149. Rouse, W.; Haas, R.H. Monitoring vegetation systems in the Great Plains with ERTS. *Proc. Third Earth Resour. Technol. Satell. 1 Symp.* **1974**, *9*, 301–317.
150. Huete, A.; Didan, K.; Miura, T.; Rodriguez, E.P.; Gao, X.; Ferreira, L.G. Overview of the radiometric and biophysical performance of the MODIS vegetation indices. *Remote Sens. Environ.* **2002**, *83*, 195–213. [CrossRef]
151. Qi, J.; Chehbouni, A.; Huete, A.R.; Kerr, Y.H.; Sorooshian, S. A modified soil adjusted vegetation index. *Remote Sens. Environ.* **1994**, *48*, 119–126. [CrossRef]
152. Richardson, A.J.; Wiegand, C.L. Distinguishing Vegetation from Soil Background Information. *Photogramm. Eng. Remote Sens.* **1977**, *43*, 1541–1552.
153. Haboudane, D. Hyperspectral vegetation indices and novel algorithms for predicting green LAI of crop canopies: Modeling and validation in the context of precision agriculture. *Remote Sens. Environ.* **2004**, *90*, 337–352. [CrossRef]
154. Baret, F.; Jacquemoud, S.; Hanocq, J.F. About the soil line concept in remote sensing. *Adv. Space Res.* **1993**, *13*, 281–284. [CrossRef]
155. Batten, G.D. Plant analysis using near infrared reflectance spectroscopy: The potential and the limitations. *Aust. J. Exp. Agric.* **1998**, *38*, 697–706. [CrossRef]
156. Jiang, Z.; Huete, A.; Didan, K.; Miura, T. Development of a two-band enhanced vegetation index without a blue band. *Remote Sens. Environ.* **2008**, *112*, 3833–3845. [CrossRef]
157. Daughtry, C. Estimating Corn Leaf Chlorophyll Concentration from Leaf and Canopy Reflectance. *Remote Sens. Environ.* **2000**, *74*, 229–239. [CrossRef]
158. OwenSmith, N. Ecological guidelines for waterpoints in extensive protected areas. *S. Afr. J. Wildl. Res.* **1996**, *26*, 107–112.
159. Smit, I.P.J.; Grant, C.C.; Devereux, B.J. Do artificial waterholes influence the way herbivores use the landscape? Herbivore distribution patterns around rivers and artificial surface water sources in a large African savanna park. *Biol. Conserv.* **2007**, *136*, 85–99. [CrossRef]
160. Ryan, S.J.; Knechtel, C.U.; Getz, W.M. Range and Habitat Selection of African Buffalo in South Africa. *J. Wildl. Manag.* **2006**, *70*, 764–776. [CrossRef]
161. Hunter, C.G. Land uses on the Botswana/Zimbabwe border and their effects on buffalo. *S. Afr. J. Wildl. Res.* **1996**, *26*, 136–150.
162. Western, D. Water availability and its influence on the structure and dynamics of a savannah large mammal community. *Afr. J. Ecol.* **1975**, *13*, 265–286. [CrossRef]
163. Cornélis, D.; Melletti, M.; Korte, L.; Ryan, S.J.; Mirabile, M.; Prin, T.; Prins, H. African Buffalo (Syncerus Caffer Sparrman, 1779). Available online: http://agritrop.cirad.fr/578582/ (accessed on 28 July 2020).
164. Moyo, B.; Dube, S.; Lesoli, M.; Masika, P. Seasonal habitat use and movement patterns of cattle grazing different rangeland types in the communal areas of the Eastern Cape, South Africa. *Afr. J. Agric. Res.* **2013**, *8*, 36–45. [CrossRef]
165. Scoones, I. Exploiting heterogeneity:habitat use by cattle in dryland Zimbabwe. *J. Arid Environ.* **1995**, *29*, 221–237. [CrossRef]
166. Bennitt, E.; Bonyongo, M.C.; Harris, S. Habitat Selection by African Buffalo (Syncerus caffer) in Response to Landscape-Level Fluctuations in Water Availability on Two Temporal Scales. *PLoS ONE* **2014**, *9*, e101346. [CrossRef]
167. Redfern, J.V.; Grant, R.; Biggs, H.; Getz, W.M. Surface water constraints on herbivore foraging in the Kruger National Park, South Africa. *Ecology* **2003**, *84*, 2092–2107. [CrossRef]
168. Traill, L.W.; Bigalke, R.C. A presence-only habitat suitability model for large grazing African ungulates and its utility for wildlife management. *Afr. J. Ecol.* **2007**, *45*, 347–354. [CrossRef]
169. Fritz, H.; Garine-Wichatitsky, M.D.; Letessier, G. Habitat Use by Sympatric Wild and Domestic Herbivores in an African Savanna Woodland: The Influence of Cattle Spatial Behaviour. *J. Appl. Ecol.* **1996**, *33*, 589. [CrossRef]

170. Georgiadis, N.J.; Ihwagi, F.; Olwero, J.G.N.; Romañach, S.S. Savanna herbivore dynamics in a livestock-dominated landscape. II: Ecological, conservation, and management implications of predator restoration. *Biol. Conserv.* **2007**, *137*, 473–483. [CrossRef]
171. Huang, C.; Chen, Y.; Zhang, S.; Wu, J. Detecting, Extracting, and Monitoring Surface Water From Space Using Optical Sensors: A Review. *Rev. Geophys.* **2018**, *56*, 333–360. [CrossRef]
172. Majozi, N.P.; Mannaerts, C.M.; Ramoelo, A.; Mathieu, R.; Nickless, A.; Verhoef, W. Analysing surface energy balance closure and partitioning over a semi-arid savanna FLUXNET site in Skukuza, Kruger National Park, South Africa. *Hydrol. Earth Syst. Sci.* **2017**, *21*, 3401–3415. [CrossRef]
173. Donchyts, G.; Baart, F.; Winsemius, H.; Gorelick, N.; Kwadijk, J.; van de Giesen, N. Earth's surface water change over the past 30 years. *Nat. Clim. Chang.* **2016**, *6*, 810. [CrossRef]
174. Huang, C.; Chen, Y.; Wu, J.; Li, L.; Liu, R. An evaluation of Suomi NPP-VIIRS data for surface water detection. *Remote Sens. Lett.* **2015**, *6*, 155–164. [CrossRef]
175. Ramoelo, A.; Majozi, N.; Mathieu, R.; Jovanovic, N.; Nickless, A.; Dzikiti, S. Validation of Global Evapotranspiration Product (MOD16) using Flux Tower Data in the African Savanna, South Africa. *Remote Sens.* **2014**, *6*, 7406–7423. [CrossRef]
176. Alsdorf, D.E.; Rodríguez, E.; Lettenmaier, D.P. Measuring surface water from space. *Rev. Geophys.* **2007**, 45. [CrossRef]
177. Soti, V.; Puech, C.; Lo Seen, D.; Bertran, A.; Vignolles, C.; Mondet, B.; Dessay, N.; Tran, A. The potential for remote sensing and hydrologic modelling to assess the spatio-temporal dynamics of ponds in the Ferlo Region (Senegal). *Hydrol. Earth Syst. Sci.* **2010**, *14*, 1449–1464. [CrossRef]
178. Acharya, T.; Lee, D.; Yang, I.; Lee, J. Identification of Water Bodies in a Landsat 8 OLI Image Using a J48 Decision Tree. *Sensors* **2016**, *16*, 1075. [CrossRef]
179. Sun, D.; Yu, Y.; Goldberg, M.D. Deriving Water Fraction and Flood Maps From MODIS Images Using a Decision Tree Approach. *IEEE J. Sel. Top. Appl. Earth Obs. Remote Sens.* **2011**, *4*, 814–825. [CrossRef]
180. Frazier, P.S.; Page, K.J. Water Body Detection and Delineation with Landsat TM Data. *Photogramm. Eng. Remote Sens.* **2000**, *12*, 1461–1467.
181. Mohammadi, A.; Costelloe, J.F.; Ryu, D. Application of time series of remotely sensed normalized difference water, vegetation and moisture indices in characterizing flood dynamics of large-scale arid zone floodplains. *Remote Sens. Environ.* **2017**, *190*, 70–82. [CrossRef]
182. Chen, Y.; Wang, B.; Pollino, C.A.; Cuddy, S.M.; Merrin, L.E.; Huang, C. Estimate of flood inundation and retention on wetlands using remote sensing and GIS: Spatial modeliing of flood inundation and retention on wetlands. *Ecohydrology* **2014**. [CrossRef]
183. Huang, C.; Chen, Y.; Wu, J. DEM-based modification of pixel-swapping algorithm for enhancing floodplain inundation mapping. *Int. J. Remote Sens.* **2014**, *35*, 365–381. [CrossRef]
184. Owen, H.J.F.; Duncan, C.; Pettorelli, N. Testing the water: Detecting artificial water points using freely available satellite data and open source software. *Remote Sens. Ecol. Conserv.* **2015**, *1*, 61–72. [CrossRef]
185. Hardisky, M.; Klemas, V.; Smart, R. The Influence of Soil-Salinity, Growth Form, and Leaf Moisture on the Spectral Radiance of Spartina-Alterniflora Canopies. *Photogramm. Eng. Remote Sens.* **1983**, *49*, 77–83.
186. McFeeters, S.K. The use of the Normalized Difference Water Index (NDWI) in the delineation of open water features. *Int. J. Remote Sens.* **1996**, *17*, 1425–1432. [CrossRef]
187. Gao, B. NDWI—A normalized difference water index for remote sensing of vegetation liquid water from space. *Remote Sens. Environ.* **1996**, *58*, 257–266. [CrossRef]
188. Lacaux, J.P.; Tourre, Y.M.; Vignolles, C.; Ndione, J.A.; Lafaye, M. Classification of ponds from high-spatial resolution remote sensing: Application to Rift Valley Fever epidemics in Senegal. *Remote Sens. Environ.* **2007**, *106*, 66–74. [CrossRef]
189. Clandillon, S.; Fraipont, P.; Yesou, H. Assessment of the future SPOT 4 MIR for wetland monitoring and soil moisture analysis: Simulation over the Ried Center Alsace (France). In Proceedings of the Remote Sensing for Agriculture, Forestry, and Natural Resources, International Society for Optics and Photonics, Paris, France, 1 January 1995; Volume 2585, pp. 102–111.
190. Feyisa, G.L.; Meilby, H.; Fensholt, R.; Proud, S.R. Automated Water Extraction Index: A new technique for surface water mapping using Landsat imagery. *Remote Sens. Environ.* **2014**, *140*, 23–35. [CrossRef]
191. Fisher, A.; Flood, N.; Danaher, T. Comparing Landsat water index methods for automated water classification in eastern Australia. *Remote Sens. Environ.* **2016**, *175*, 167–182. [CrossRef]

192. Jin, H.; Huang, C.; Lang, M.W.; Yeo, I.-Y.; Stehman, S.V. Monitoring of wetland inundation dynamics in the Delmarva Peninsula using Landsat time-series imagery from 1985 to 2011. *Remote Sens. Environ.* **2017**, *190*, 26–41. [CrossRef]
193. Bioresita, F.; Puissant, A.; Stumpf, A.; Malet, J.-P. A Method for Automatic and Rapid Mapping of Water Surfaces from Sentinel-1 Imagery. *Remote Sens.* **2018**, *10*, 217. [CrossRef]
194. Chapman, B.; McDonald, K.; Shimada, M.; Rosenqvist, A.; Schroeder, R.; Hess, L. Mapping Regional Inundation with Spaceborne L-Band SAR. *Remote Sens.* **2015**, *7*, 5440–5470. [CrossRef]
195. Martinis, S.; Twele, A.; Voigt, S. Unsupervised Extraction of Flood-Induced Backscatter Changes in SAR Data Using Markov Image Modeling on Irregular Graphs. *IEEE Trans. Geosci. Remote Sens.* **2011**, *49*, 251–263. [CrossRef]
196. Bartsch, A.; Trofaier, A.M.; Hayman, G.; Sabel, D.; Schlaffer, S.; Clark, D.B.; Blyth, E. Detection of open water dynamics with ENVISAT ASAR in support of land surface modelling at high latitudes. *Biogeosciences* **2012**, *9*, 703–714. [CrossRef]
197. Martinis, S.; Twele, A.; Voigt, S. Towards operational near real-time flood detection using a split-based automatic thresholding procedure on high resolution TerraSAR-X data. *Nat. Hazards Earth Syst. Sci.* **2009**, *9*, 303–314. [CrossRef]
198. Simon, R.N.; Tormos, T.; Danis, P.A. Geographic Object Based Image Analysis Using very High Spatial and Temporal Resolution Radar and Optical Imagery in Tracking Water Level Fluctuations in a Freshwater Reservoir. *South-Eastern Eur. J. Earth Obs. Geomat.* **2014**, *3*, 287–291.
199. Evans, T.L.; Costa, M.; Silva, T.S.F.; Telmer, K. Using PALSAR and RADARSAT-2 to map land cover andinundation in the Brazilian Pantanal. In Proceedings of the 3e Simpósio de Geotecnologias no Pantanal, Caceres, Brazil, 16–20 October 2010; pp. 485–494.
200. Mitchell, A.L.; Milne, A.K.; Tapley, I. Towards an operational SAR monitoring system for monitoring environmental flows in the Macquarie Marshes. *Wetl. Ecol. Manag.* **2015**, *23*, 61–77. [CrossRef]
201. Martinez, J.; Letoan, T. Mapping of flood dynamics and spatial distribution of vegetation in the Amazon floodplain using multitemporal SAR data. *Remote Sens. Environ.* **2007**, *108*, 209–223. [CrossRef]
202. Twele, A.; Cao, W.; Plank, S.; Martinis, S. Sentinel-1-based flood mapping: A fully automated processing chain. *Int. J. Remote Sens.* **2016**, *37*, 2990–3004. [CrossRef]
203. Martinis, S.; Kuenzer, C.; Wendleder, A.; Huth, J.; Twele, A.; Roth, A.; Dech, S. Comparing four operational SAR-based water and flood detection approaches. *Int. J. Remote Sens.* **2015**, *36*, 3519–3543. [CrossRef]
204. Westerhoff, R.S.; Kleuskens, M.P.H.; Winsemius, H.C.; Huizinga, H.J.; Brakenridge, G.R.; Bishop, C. Automated global water mapping based on wide-swath orbital synthetic-aperture radar. *Hydrol. Earth Syst. Sci.* **2013**, *17*, 651–663. [CrossRef]
205. Brisco, B.; Short, N. A semi-automated tool for surface water mapping with RADARSAT-. *Can. J. Remote Sens.* **2009**, *35*, 9.
206. Schumann, G.; Bates, P.D.; Horritt, M.S.; Matgen, P.; Pappenberger, F. Progress in integration of remote sensing–derived flood extent and stage data and hydraulic models. *Rev. Geophys.* **2009**, *47*, RG4001. [CrossRef]
207. Bertram, A.; Wendleder, A.; Schmitt, A.; Huber, M. Long-term monitoring of water dynamics in the Sahel region using the Multi-SAR-System. *ISPRS Int. Arch. Photogramm. Remote Sens. Spat. Inf. Sci.* **2016**, *XLI-B8*, 313–320. [CrossRef]
208. Haas, E.M.; Bartholomé, E.; Lambin, E.F.; Vanacker, V. Remotely sensed surface water extent as an indicator of short-term changes in ecohydrological processes in sub-Saharan Western Africa. *Remote Sens. Environ.* **2011**, *115*, 3436–3445. [CrossRef]
209. Moser, L.; Voigt, S.; Schoepfer, E.; Palmer, S. Multitemporal Wetland Monitoring in Sub-Saharan West-Africa Using Medium Resolution Optical Satellite Data. *IEEE J. Sel. Top. Appl. Earth Obs. Remote Sens.* **2014**, *7*, 3402–3415. [CrossRef]
210. Rokni, K.; Ahmad, A.; Solaimani, K.; Hazini, S. A new approach for surface water change detection: Integration of pixel level image fusion and image classification techniques. *Int. J. Appl. Earth Obs. Geoinf.* **2015**, *34*, 226–234. [CrossRef]
211. Du, Y.; Zhang, Y.; Ling, F.; Wang, Q.; Li, W.; Li, X. Water Bodies' Mapping from Sentinel-2 Imagery with Modified Normalized Difference Water Index at 10-m Spatial Resolution Produced by Sharpening the SWIR Band. *Remote Sens.* **2016**, *8*, 354. [CrossRef]

212. Dzinotizei, Z.; Murwira, A.; Zengeya, F.M.; Guerrini, L. Mapping waterholes and testing for aridity using a remote sensing water index in a southern African semi-arid wildlife area. *Geocarto Int.* **2018**, *33*, 1268–1280. [CrossRef]
213. Zvidzai, M.; Murwira, A.; Caron, A. Waterhole use patterns at the wildlife/livestock interface in a semi-arid savanna of Southern Africa. *Int. J. Dev. Sustain.* **2013**, *17*, 455–471.
214. Crosmary, W.-G.; Valeix, M.; Fritz, H.; Madzikanda, H.; Côté, S.D. African ungulates and their drinking problems: Hunting and predation risks constrain access to water. *Anim. Behav.* **2012**, *83*, 145–153. [CrossRef]
215. Chamaillé-Jammes, S.; Fritz, H.; Murindagomo, F. Climate-driven fluctuations in surface-water availability and the buffering role of artificial pumping in an African savanna: Potential implication for herbivore dynamics. *Austral Ecol.* **2007**, *32*, 740–748. [CrossRef]
216. Chamaillé-Jammes, S.; Charbonnel, A.; Dray, S.; Madzikanda, H.; Fritz, H. Spatial Distribution of a Large Herbivore Community at Waterholes: An Assessment of Its Stability over Years in Hwange National Park, Zimbabwe. *PLoS ONE* **2016**, *11*, e0153639. [CrossRef]
217. Pekel, J.-F.; Cottam, A.; Gorelick, N.; Belward, A.S. High-resolution mapping of global surface water and its long-term changes. *Nature* **2016**, *540*, 418–422. [CrossRef]
218. Lamarche, C.; Santoro, M.; Bontemps, S.; d'Andrimont, R.; Radoux, J.; Giustarini, L.; Brockmann, C.; Wevers, J.; Defourny, P.; Arino, O. Compilation and Validation of SAR and Optical Data Products for a Complete and Global Map of Inland/Ocean Water Tailored to the Climate Modeling Community. *Remote Sens.* **2017**, *9*, 36. [CrossRef]
219. Lehner, B.; Döll, P. Development and validation of a global database of lakes, reservoirs and wetlands. *J. Hydrol.* **2004**, *296*, 1–22. [CrossRef]
220. Slater, J.A.; Garvey, G.; Johnston, C.; Haase, J.; Heady, B.; Kroenung, G.; Little, J. The SRTM Data "Finishing" Process and Products. *Photogramm. Eng. Remote Sens.* **2006**, *72*, 237–247. [CrossRef]
221. Santoro, M.; Wegmuller, U. Multi-temporal Synthetic Aperture Radar Metrics Applied to Map Open Water Bodies. *IEEE J. Sel. Top. Appl. Earth Obs. Remote Sens.* **2014**, *7*, 3225–3238. [CrossRef]
222. Carroll, M.L.; Townshend, J.R.; DiMiceli, C.M.; Noojipady, P.; Sohlberg, R.A. A new global raster water mask at 250 m resolution. *Int. J. Digit. Earth* **2009**, *2*, 291–308. [CrossRef]
223. Lacaze, R.; Smets, B.; Baret, F.; Weiss, M.; Ramon, D.; Montersleet, B.; Wandrebeck, L.; Calvet, J.-C.; Roujean, J.-L.; Camacho, F. Operational 333m biophysical products of the Copernicus Global Land Service For Agriculture Monitoring. *Isprs Int. Arch. Photogramm. Remote Sens. Spat. Inf. Sci.* **2015**, *XL-7/W3*, 53–56. [CrossRef]
224. Yamazaki, D.; Trigg, M.A.; Ikeshima, D. Development of a global ~90m water body map using multi-temporal Landsat images. *Remote Sens. Environ.* **2015**, *171*, 337–351. [CrossRef]
225. Goldammer, J.G.; Ronde, C.D. *Wildland Fire Management Handbook for Sub-Sahara Africa*; African Minds: Cape Town, South Africa, 2004; ISBN 978-1-919833-65-1.
226. Bailey, A.W. Understanding Fire Ecology for Range Management. In *Vegetation Science Applications for Rangeland Analysis and Management*; Tueller, P.T., Ed.; Handbook of vegetation science; Springer: Dordrecht, The Netherlands, 1988; pp. 527–557. ISBN 978-94-009-3085-8.
227. Higgins, S.I.; Bond, W.J.; February, E.C.; Bronn, A.; Euston-Brown, D.I.W.; Enslin, B.; Govender, N.; Rademan, L.; O'Regan, S.; Potgieter, A.L.F.; et al. Effects of four decades of fire manipulation on woody vegetation savanna. *Ecology* **2007**, *88*, 1119–1125. [CrossRef]
228. Hopcraft, J.G.C.; Sinclair, A.R.E.; Packer, C. Planning for success: Serengeti lions seek prey accessibility rather than abundance. *J. Anim. Ecol.* **2005**, *74*, 559–566. [CrossRef]
229. Archibald, S.; Bond, W.J. Grazer movements: Spatial and temporal responses to burning in a tall-grass African savanna. *Int. J. Wildland Fire* **2004**, *13*, 377–385. [CrossRef]
230. Odadi, W.O.; Kimuyu, D.M.; Sensenig, R.L.; Veblen, K.E.; Riginos, C.; Young, T.P. Fire-induced negative nutritional outcomes for cattle when sharing habitat with native ungulates in an African savanna. *J. Appl. Ecol.* **2017**, *54*, 935–944. [CrossRef]
231. Meng, R.; Dennison, P.E.; Huang, C.; Moritz, M.A.; D'Antonio, C. Effects of fire severity and post-fire climate on short-term vegetation recovery of mixed-conifer and red fir forests in the Sierra Nevada Mountains of California. *Remote Sens. Environ.* **2015**, *171*, 311–325. [CrossRef]

232. Lentile, L.B.; Holden, Z.A.; Smith, A.M.S.; Falkowski, M.J.; Hudak, A.T.; Morgan, P.; Lewis, S.A.; Gessler, P.E.; Benson, N.C. Remote sensing techniques to assess active fire characteristics and post-fire effects. *Int. J. Wildland Fire* **2006**, *15*, 319. [CrossRef]
233. Turner, M.G.; Romme, W.H.; Gardner, R.H. Prefire heterogeneity, fire severity, and early postfire plant reestablishment in subalpine forests of Yellowstone National Park, Wyoming. *Int. J. Wildland Fire* **1999**, *9*, 21. [CrossRef]
234. Meng, R.; Zhao, F. Remote Sensing of Fire Effects. In *Remote Sensing of Hydrometeorological Hazards*; Petropoulos, G.P., Islam, T., Eds.; CRC Press: Boca Raton, FL, USA, 2017; pp. 261–283. ISBN 1-351-65071-1.
235. Leblon, B.; Bourgeau-Chavez, L.; San-Miguel-Ayanz, J. Use of Remote Sensing in Wildfire Management. In *Sustainable Development—Authoritative and Leading Edge Content for Environmental Management*; Curkovic, S., Ed.; InTech: Rijeka, Croatia, 2012; ISBN 978-953-51-0682-1.
236. Morgan, P.; Keane, R.E.; Dillon, G.K.; Jain, T.B.; Hudak, A.T.; Karau, E.C.; Sikkink, P.G.; Holden, Z.A.; Strand, E.K. Challenges of assessing fire and burn severity using field measures, remote sensing and modelling. *Int. J. Wildland Fire* **2014**, *23*, 1045. [CrossRef]
237. Chu, T.; Guo, X. Remote Sensing Techniques in Monitoring Post-Fire Effects and Patterns of Forest Recovery in Boreal Forest Regions: A Review. *Remote Sens.* **2013**, *6*, 470–520. [CrossRef]
238. Schroeder, W.; Oliva, P.; Giglio, L.; Csiszar, I.A. The New VIIRS 375m active fire detection data product: Algorithm description and initial assessment. *Remote Sens. Environ.* **2014**, *143*, 85–96. [CrossRef]
239. Giglio, L. Global estimation of burned area using MODIS active fire observations. *Atmos. Chem. Phys.* **2006**, *6*, 957–974. [CrossRef]
240. Chuvieco, E.; Giglio, L.; Justice, C. Global characterization of fire activity: Toward defining fire regimes from Earth observation data. *Glob. Chang. Biol.* **2008**, *14*, 1488–1502. [CrossRef]
241. Key, C.H.; Benson, N.C. Landscape Assessment (LA). In *FIREMON: Fire effects Monitoring and Inventory System*; Gen. Tech. Rep. RMRS-GTR-164-CD.; Lutes Duncan, C., Keane Robert, E., Caratti John, F., Key Carl, H., Benson Nathan, C., Sutherland, S., Gangi Larry, J., Eds.; U.S. Department of Agriculture, Forest Service, Rocky Mountain Research Station: Fort Collins, CO, USA, 2006.
242. Quintano, C.; Fernández-Manso, A.; Fernández-Manso, O.; Shimabukuro, Y.E. Mapping burned areas in Mediterranean countries using spectral mixture analysis from a uni-temporal perspective. *Int. J. Remote Sens.* **2006**, *27*, 645–662. [CrossRef]
243. Petropoulos, G.P.; Kontoes, C.; Keramitsoglou, I. Burnt area delineation from a uni-temporal perspective based on Landsat TM imagery classification using Support Vector Machines. *Int. J. Appl. Earth Obs. Geoinf.* **2011**, *13*, 70–80. [CrossRef]
244. Hudak, A.T.; Brockett, B.H. Mapping fire scars in a southern African savannah using Landsat imagery. *Int. J. Remote Sens.* **2004**, *25*, 3231–3243. [CrossRef]
245. Goodwin, N.R.; Collett, L.J. Development of an automated method for mapping fire history captured in Landsat TM and ETM+ time series across Queensland, Australia. *Remote Sens. Environ.* **2014**, *148*, 206–221. [CrossRef]
246. Kennedy, R.E.; Yang, Z.; Braaten, J.; Copass, C.; Antonova, N.; Jordan, C.; Nelson, P. Attribution of disturbance change agent from Landsat time-series in support of habitat monitoring in the Puget Sound region, USA. *Remote Sens. Environ.* **2015**, *166*, 271–285. [CrossRef]
247. Zhao, F.; Huang, C.; Zhu, Z. Use of Vegetation Change Tracker and Support Vector Machine to Map Disturbance Types in Greater Yellowstone Ecosystems in a 1984–2010 Landsat Time Series. *IEEE Geosci. Remote Sens. Lett.* **2015**, *12*, 1650–1654. [CrossRef]
248. Giglio, L.; Loboda, T.; Roy, D.P.; Quayle, B.; Justice, C.O. An active-fire based burned area mapping algorithm for the MODIS sensor. *Remote Sens. Environ.* **2009**, *113*, 408–420. [CrossRef]
249. Lizundia-Loiola, J.; Otón, G.; Ramo, R.; Chuvieco, E. A spatio-temporal active-fire clustering approach for global burned area mapping at 250 m from MODIS data. *Remote Sens. Environ.* **2020**, *236*, 111493. [CrossRef]
250. Boschetti, L.; Roy, D.P.; Justice, C.O.; Humber, M.L. MODIS–Landsat fusion for large area 30m burned area mapping. *Remote Sens. Environ.* **2015**, *161*, 27–42. [CrossRef]
251. Klerk, D.; Margaret, H. *A Pragmatic Assessment of the Usefulness of the MODIS (Terra and Aqua) 1-km Active Fire (MOD14A2 and MYD14A2) Products for Mapping Fires in the Fynbos Biome*; CSIRO Publishing: Victoria, Australia, 2008.

252. Justice, C.O.; Giglio, L.; Korontzi, S.; Owens, J.; Morisette, J.T.; Roy, D.; Descloitres, J.; Alleaume, S.; Petitcolin, F.; Kaufman, Y. The MODIS fire products. *Remote Sens. Environ.* **2002**, *83*, 244–262. [CrossRef]
253. Roy, D.P.; Boschetti, L.; Justice, C.O.; Ju, J. The collection 5 MODIS burned area product—Global evaluation by comparison with the MODIS active fire product. *Remote Sens. Environ.* **2008**, *112*, 3690–3707. [CrossRef]
254. Schroeder, D.W. Visible Infrared Imaging Radiometer Suite (VIIRS) 375 m & 750 m Active Fire Detection Data Sets Based on NASA VIIRS Land Science Investigator Processing System (SIPS) Reprocessed Data—Version 1. 2017. Available online: https://lpdaac.usgs.gov/documents/132/VNP14_User_Guide_v1.3.pdf (accessed on 2 August 2019).
255. Wooster, M.J.; Xu, W.; Nightingale, T. Sentinel-3 SLSTR active fire detection and FRP product: Pre-launch algorithm development and performance evaluation using MODIS and ASTER datasets. *Remote Sens. Environ.* **2011**, *120*, 236–254. [CrossRef]
256. Li, Z.; Nadon, S.; Cihlar, J. Satellite-based detection of Canadian boreal forest fires: Development and application of the algorithm. *Int. J. Remote Sens.* **2000**, *21*, 3057–3069. [CrossRef]
257. Chuvieco, E.; Yue, C.; Heil, A.; Mouillot, F.; Alonso-Canas, I.; Padilla, M.; Pereira, J.M.; Oom, D.; Tansey, K. A new global burned area product for climate assessment of fire impacts: A new global burned area product. *Glob. Ecol. Biogeogr.* **2016**, *25*, 619–629. [CrossRef]
258. Lutes, D.C.; Keane, R.E.; Caratti, J.F.; Key, C.H.; Benson, N.C.; Sutherland, S.; Gangi, L.J. *FIREMON: Fire Effects Monitoring and Inventory System*; U.S. Department of Agriculture, Forest Service, Rocky Mountain Research Station: Ft. Collins, CO, USA, 2006; p. RMRS-GTR-164.
259. Chuvieco, E.; Martín, M.P.; Palacios, A. Assessment of different spectral indices in the red-near-infrared spectral domain for burned land discrimination. *Int. J. Remote Sens.* **2002**, *23*, 5103–5110. [CrossRef]
260. Trigg, S.; Flasse, S. An evaluation of different bi-spectral spaces for discriminating burned shrub-savannah. *Int. J. Remote Sens.* **2001**, *22*, 2641–2647. [CrossRef]
261. Smith, A.M.S.; Wooster, M.J.; Drake, N.A.; Dipotso, F.M.; Falkowski, M.J.; Hudak, A.T. Testing the potential of multi-spectral remote sensing for retrospectively estimating fire severity in African Savannahs. *Remote Sens. Environ.* **2005**, *97*, 92–115. [CrossRef]
262. Holden, Z.A.; Smith, A.M.S.; Morgan, P.; Rollins, M.G.; Gessler, P.E. Evaluation of novel thermally enhanced spectral indices for mapping fire perimeters and comparisons with fire atlas data. *Int. J. Remote Sens.* **2005**, *26*, 4801–4808. [CrossRef]
263. Smith, A.M.S.; Drake, N.A.; Wooster, M.J.; Hudak, A.T.; Holden, Z.A.; Gibbons, C.J. Production of Landsat ETM+ reference imagery of burned areas within Southern African savannahs: Comparison of methods and application to MODIS. *Int. J. Remote Sens.* **2007**, *28*, 2753–2775. [CrossRef]
264. Galvin, K.A. Transitions: Pastoralists Living with Change. *Annu. Rev. Anthr.* **2009**, *38*, 185–198. [CrossRef]
265. Dodman, T.; Diagana, C. Movements of waterbirds within Africa and their conservation implications. *Ostrich* **2007**, *78*, 149–154. [CrossRef]
266. Conybeare, A. Buffalo numbers, home range and daily movement in the Sengua Wildlife Research Area, Zimbabwe. *S. Afr. J. Wildl. Res. 24 Mon. Delayed Open Access* **1981**, *11*, 89–93.
267. Funston, P.J.; Skinner, J.D.; Dott, H.M. Seasonal variation in movement patterns, home range and habitat selection of buffaloes in a semi-arid habitat. *Afr. J. Ecol.* **1994**, *32*, 100–114. [CrossRef]
268. Sinclair, A.R.E. The African Buffalo. In *A Study of Resource Limitation of Populations*; University of Chicago Press: Chicago, NY, USA, 1977.
269. Bennett, J.; Lent, P.; Harris, P. Dry season foraging preferences of cattle and sheep in a communal area of South Africa. *Afr. J. Range Forage Sci.* **2007**, *24*, 109–121. [CrossRef]
270. Heaney, A.; Little, E.; Ng, S.; Shaman, J. Meteorological variability and infectious disease in Central Africa: A review of meteorological data quality: Meteorology and infectious disease in C. Africa. *Ann. N. Y. Acad. Sci.* **2016**, *1382*, 31–43. [CrossRef] [PubMed]
271. Pfeifroth, U.; Trentmann, J.; Fink, A.H.; Ahrens, B. Evaluating Satellite-Based Diurnal Cycles of Precipitation in the African Tropics. *J. Appl. Meteor. Clim.* **2016**, *55*, 23–39. [CrossRef]
272. Toté, C.; Patricio, D.; Boogaard, H.; van der Wijngaart, R.; Tarnavsky, E.; Funk, C. Evaluation of Satellite Rainfall Estimates for Drought and Flood Monitoring in Mozambique. *Remote Sens.* **2015**, *7*, 1758–1776. [CrossRef]

273. Maidment, R.I.; Grimes, D.I.F.; Allan, R.P.; Greatrex, H.; Rojas, O.; Leo, O. Evaluation of satellite-based and model re-analysis rainfall estimates for Uganda: Evaluation of rainfall estimates for Uganda. *Met. Apps* **2013**, *20*, 308–317. [CrossRef]
274. Thiemig, V.; Rojas, R.; Zambrano-Bigiarini, M.; Levizzani, V.; De Roo, A. Validation of Satellite-Based Precipitation Products over Sparsely Gauged African River Basins. *J. Hydrometeor.* **2012**, *13*, 1760–1783. [CrossRef]
275. Roca, R.; Chambon, P.; Jobard, I.; Kirstetter, P.-E.; Gosset, M.; Bergès, J.C. Comparing Satellite and Surface Rainfall Products over West Africa at Meteorologically Relevant Scales during the AMMA Campaign Using Error Estimates. *J. Appl. Meteor. Clim.* **2010**, *49*, 715–731. [CrossRef]
276. Dinku, T.; Chidzambwa, S.; Ceccato, P.; Connor, S.J.; Ropelewski, C.F. Validation of high-resolution satellite rainfall products over complex terrain. *Int. J. Remote Sens.* **2008**, *29*, 4097–4110. [CrossRef]
277. Grimes, D.I.F.; Pardo-Igúzquiza, E.; Bonifacio, R. Optimal areal rainfall estimation using raingauges and satellite data. *J. Hydrol.* **1999**, *222*, 93–108. [CrossRef]
278. Laurent, H.; Jobard, I.; Toma, A. Validation of satellite and ground-based estimates of precipitation over the Sahel. *Atmos. Res.* **1998**, *47–48*, 651–670. [CrossRef]
279. Xie, P.; Janowiak, J.E.; Arkin, P.A.; Adler, R.; Gruber, A.; Ferraro, R.; Huffman, G.J.; Curtis, S. GPCP Pentad Precipitation Analyses: An Experimental Dataset Based on Gauge Observations and Satellite Estimates. *J. Clim.* **2003**, *16*, 2197–2214. [CrossRef]
280. Huffman, G.; Adler, R.; Rudolf, B.; Schneider, U.; Keehn, P. Global Precipitation Estimates Based on a Technique for Combining Satellite-Based Estimates, Rain-Gauge Analysis, and Nwp Model Precipitation Information. *J. Clim.* **1995**, *8*, 1284–1295. [CrossRef]
281. Camberlin, P.; Barraud, G.; Bigot, S.; Dewitte, O.; Makanzu Imwangana, F.; Maki Mateso, J.; Martiny, N.; Monsieurs, E.; Moron, V.; Pellarin, T.; et al. Evaluation of remotely sensed rainfall products over Central Africa. *Q. J. R. Meteorol. Soc.* **2019**, qj.3547. [CrossRef]
282. Dembélé, M.; Zwart, S.J. Evaluation and comparison of satellite-based rainfall products in Burkina Faso, West Africa. *Int. J. Remote Sens.* **2016**, *37*, 3995–4014. [CrossRef]
283. Bayissa, Y.; Tadesse, T.; Demisse, G.; Shiferaw, A. Evaluation of Satellite-Based Rainfall Estimates and Application to Monitor Meteorological Drought for the Upper Blue Nile Basin, Ethiopia. *Remote Sens.* **2017**, *9*, 669. [CrossRef]
284. Seyama, E.S.; Masocha, M.; Dube, T. Evaluation of TAMSAT satellite rainfall estimates for southern Africa: A comparative approach. *Phys. Chem. Earth Parts A B C* **2019**, *112*, 141–153. [CrossRef]
285. Villarini, G.; Mandapaka, P.V.; Krajewski, W.F.; Moore, R.J. Rainfall and sampling uncertainties: A rain gauge perspective. *J. Geophys. Res. Atmos.* **2008**, 113. [CrossRef]
286. Maidment, R.I.; Allan, R.P.; Black, E. Recent observed and simulated changes in precipitation over Africa. *Geophys. Res. Lett.* **2015**, *42*, 8155–8164. [CrossRef]
287. Sylla, M.B.; Giorgi, F.; Coppola, E.; Mariotti, L. Uncertainties in daily rainfall over Africa: Assessment of gridded observation products and evaluation of a regional climate model simulation. *Int. J. Climatol.* **2013**, *33*, 1805–1817. [CrossRef]
288. Huffman, G.J.; Bolvin, D.T.; Nelkin, E.J.; Wolff, D.B.; Adler, R.F.; Gu, G.; Hong, Y.; Bowman, K.P.; Stocker, E.F. The TRMM Multisatellite Precipitation Analysis (TMPA): Quasi-Global, Multiyear, Combined-Sensor Precipitation Estimates at Fine Scales. *J. Hydrometeor.* **2007**, *8*, 38–55. [CrossRef]
289. Ashouri, H.; Hsu, K.-L.; Sorooshian, S.; Braithwaite, D.K.; Knapp, K.R.; Cecil, L.D.; Nelson, B.R.; Prat, O.P. PERSIANN-CDR: Daily Precipitation Climate Data Record from Multisatellite Observations for Hydrological and Climate Studies. *Bull. Amer. Meteor. Soc.* **2015**, *96*, 69–83. [CrossRef]
290. Huffman, G.J.; Adler, R.F.; Morrissey, M.M.; Bolvin, D.T.; Curtis, S.; Joyce, R.; Mcgavock, B.; Susskind, J. Global Precipitation at One-Degree Daily Resolution from Multisatellite Observations. *J. Hydrometeorol.* **2001**, *2*, 15. [CrossRef]
291. Adler, R.F.; Huffman, G.J.; Chang, A.; Ferraro, R.; Xie, P.-P.; Janowiak, J.; Rudolf, B.; Schneider, U.; Curtis, S.; Bolvin, D.; et al. The Version-2 Global Precipitation Climatology Project (GPCP) Monthly Precipitation Analysis (1979–Present). *J. Hydrometeorol.* **2003**, *4*, 21. [CrossRef]
292. Hou, D.; Charles, M.; Luo, Y.; Toth, Z.; Zhu, Y.; Krzysztofowicz, R.; Lin, Y.; Xie, P.; Seo, D.-J.; Pena, M.; et al. Climatology-Calibrated Precipitation Analysis at Fine Scales: Statistical Adjustment of Stage IV toward CPC Gauge-Based Analysis. *J. Hydrometeorol.* **2014**, *15*, 2542–2557. [CrossRef]

293. Xie, P.; Arkin, P.A. Global Precipitation: A 17-Year Monthly Analysis Based on Gauge Observations, Satellite Estimates, and Numerical Model Outputs. *Bull. Am. Meteorol. Soc.* **1997**, *78*, 20. [CrossRef]
294. Joyce, R.J.; Janowiak, J.E.; Arkin, P.A.; Xie, P. CMORPH: A Method that Produces Global Precipitation Estimates from Passive Microwave and Infrared Data at High Spatial and Temporal Resolution. *J. Hydrometeorology* **2004**, *5*, 17. [CrossRef]
295. Bolvin, D.T.; Braithwaite, D.; Hsu, K.; Joyce, R.; Kidd, C.; Nelkin, E.J.; Sorooshian, S.; Tan, J.; Xie, P. Algorithm Theoretical Basis Document (ATBD) Version 06, NASA Global Precipitation Measurement (GPM) Integrated Multi-satellitE Retrievals for GPM (IMERG). NASA/GSFC NASA/GSFC. 2019. Available online: https://gpm.nasa.gov/sites/default/files/document_files/IMERG_ATBD_V06.pdf (accessed on 15 February 2020).
296. Beck, H.E.; Wood, E.F.; Pan, M.; Fisher, C.K.; Miralles, D.G.; van Dijk, A.I.J.M.; McVicar, T.R.; Adler, R.F. MSWEP V2 Global 3-Hourly 0.1° Precipitation: Methodology and Quantitative Assessment. *Bull. Am. Meteor. Soc.* **2019**, *100*, 473–500. [CrossRef]
297. Brocca, L.; Ciabatta, L.; Massari, C.; Moramarco, T.; Hahn, S.; Hasenauer, S.; Kidd, R.; Dorigo, W.; Wagner, W.; Levizzani, V. Soil As A Natural Rain Gauge: Estimating Global Rainfall from Satellite Soil Moisture Data. Available online: https://agupubs.onlinelibrary.wiley.com/doi/abs/10.1002/2014JD021489 (accessed on 27 August 2019).
298. Funk, C.; Peterson, P.; Landsfeld, M.; Pedreros, D.; Verdin, J.; Shukla, S.; Husak, G.; Rowland, J.; Harrison, L.; Hoell, A.; et al. The climate hazards infrared precipitation with stations—A new environmental record for monitoring extremes. *Sci. Data* **2015**, *2*, 150066. [CrossRef]
299. Novella, N.S.; Thiaw, W.M. African Rainfall Climatology Version 2 for Famine Early Warning Systems. *J. Appl. Meteor. Clim.* **2013**, *52*, 588–606. [CrossRef]
300. Love, T.B.; Kumar, V.; Xie, P.; Thiaw, W. A 20-Year daily Africa precipitation climatology using saellite and gauge data. In Proceedings of the 84th AMS Annual Meeting, P5.4. Conference on Applied Climatology, Seattle, WA, USA, 11–15 January 2004; pp. 5–15.
301. Bergès, J.C.; Jobard, I.; Chopin, F.; Roca, R. EPSAT-SG: A satellite method for precipitation estimation; its concepts and implementation for the AMMA experiment. *Ann. Geophys.* **2010**, *28*, 289–308. [CrossRef]
302. Heinemann, T.; Lattanzio, A.; Roveda, F. The Eumestat multi-sensor precipitation estimate (MPE). In Proceedings of the Second International Pre-cipitation Working group (IPWG) Meeting, Monterey, CA, USA, 23–27 September 2002; pp. 23–27.
303. Maidment, R.I.; Grimes, D.; Black, E.; Tarnavsky, E.; Young, M.; Greatrex, H.; Allan, R.P.; Stein, T.; Nkonde, E.; Senkunda, S.; et al. A new, long-term daily satellite-based rainfall dataset for operational monitoring in Africa. *Sci. Data* **2017**, *4*, 170063. [CrossRef] [PubMed]
304. Dinku, T.; Funk, C.; Peterson, P.; Maidment, R.; Tadesse, T.; Gadain, H.; Ceccato, P. Validation of the CHIRPS satellite rainfall estimates over eastern Africa. *Q. J. R. Meteorol. Soc.* **2018**, *144*, 292–312. [CrossRef]
305. Ogutu, J.O.; Piepho, H.-P.; Dublin, H.T.; Bhola, N.; Reid, R.S. Rainfall influences on ungulate population abundance in the Mara-Serengeti ecosystem. *J. Anim. Ecol.* **2008**, *77*, 814–829. [CrossRef]
306. Clark, B.L.; Bevanda, M.; Aspillaga, E.; Jørgensen, N.H. Bridging disciplines with training in remote sensing for animal movement: An attendee perspective. *Remote Sens. Ecol. Conserv.* **2017**, *3*, 30–37. [CrossRef]
307. Riotte-Lambert, L.; Matthiopoulos, J. Environmental Predictability as a Cause and Consequence of Animal Movement. *Trends Ecol. Evol.* **2020**, *35*, 163–174. [CrossRef]
308. Ducgin, M.J. A review of: "Ground Truth for Remote Sensing". By P. A. Bradbury and E. M. Rollin. (Nottingham: Department of Geography, The University, 1986.) Proceedings of a Remote Sensing Society workshop held on 17 April 1986. [Pp. 220.] Price £600. *Int. J. Remote Sens.* **1987**, *8*, 1075. [CrossRef]
309. Bernd, A.; Braun, D.; Ortmann, A.; Ulloa-Torrealba, Y.Z.; Wohlfart, C.; Bell, A. More than counting pixels—perspectives on the importance of remote sensing training in ecology and conservation. *Remote Sens. Ecol. Conserv.* **2017**, *3*, 38–47. [CrossRef]
310. Rocchini, D. Effects of spatial and spectral resolution in estimating ecosystem α-diversity by satellite imagery. *Remote Sens. Environ.* **2007**, *111*, 423–434. [CrossRef]
311. Defourny, P.; Schouten, L.; Bartalev, S.; Bontemps, S.; Cacetta, P.; de Wit, A.J.W.; di Bella, C.; Gérard, B.; Giri, C.; Gond, V.; et al. Accuracy Assessment of a 300 m Global Land Cover Map: The GlobCover Experience. In Proceedings of the 33rd International Symposium on Remote Sensing of Environement, Stresa, Italy, 4–8 May 2009.

312. Winnie, J.A.; Cross, P.; Getz, W. Habitat quality and heterogeneity influence distribution and behavior in African buffalo (*Syncerus caffer*). *Ecology* **2008**, *89*, 1457–1468. [CrossRef]
313. He, K.S.; Bradley, B.A.; Cord, A.F.; Rocchini, D.; Tuanmu, M.-N.; Schmidtlein, S.; Turner, W.; Wegmann, M.; Pettorelli, N. Will remote sensing shape the next generation of species distribution models? *Remote Sens. Ecol. Conserv.* **2015**, *1*, 4–18. [CrossRef]
314. Horning, N.; Robinson, J.A.; Sterling, E.J.; Spector, S.; Turner, W. *Remote Sensing for Ecology and Conservation: A Handbook of Techniques*; Oxford University Press: Oxford, UK, 2010; ISBN 978-0-19-921995-7.
315. Gibbes, C.; Adhikari, S.; Rostant, L.; Southworth, J.; Qiu, Y. Application of Object Based Classification and High Resolution Satellite Imagery for Savanna Ecosystem Analysis. *Remote Sens.* **2010**, *2*, 2748–2772. [CrossRef]
316. Paganini, M.; Petiteville, I.; Ward, S.; Dyke, G.; Harry, S.; Harry, H.; Kerblat, F. *Satellite Earth Observations in Support of The Sustainable Development Goals, Special 2018 ed.*; CEOS-ESA: Paris, France, 2018; p. 114.
317. Venter, J.A.; Watson, L.H. Feeding and habitat use of buffalo (Syncerus caffer caffer) in the Nama-Karoo, South Africa. *South Afr. J. Wildl. Res.* **2008**, *38*, 42–51. [CrossRef]
318. Zhang, X.; Goldberg, M.D.; Yu, Y. Prototype for monitoring and forecasting fall foliage coloration in real time from satellite data. *Agric. For. Meteorol.* **2012**, *158–159*, 21–29. [CrossRef]
319. White, M.A.; Nemani, R.R. Real-time monitoring and short-term forecasting of land surface phenology. *Remote Sens. Environ.* **2006**, *104*, 43–49. [CrossRef]
320. Bellón, B.; Bégué, A.; Lo Seen, D.; de Almeida, C.; Simões, M. A Remote Sensing Approach for Regional-Scale Mapping of Agricultural Land-Use Systems Based on NDVI Time Series. *Remote Sens.* **2017**, *9*, 600. [CrossRef]
321. Bégué, A.; Arvor, D.; Bellon, B.; Betbeder, J.; De Abelleyra, D.; Ferraz, R.P.D.; Lebourgeois, V.; Lelong, C.; Simões, M.; Verón, S.R. Remote Sensing and Cropping Practices: A Review. *Remote Sens.* **2018**, *10*, 99. [CrossRef]
322. Archibald, S.; Nickless, A.; Govender, N.; Scholes, R.J.; Lehsten, V. Climate and the inter-annual variability of fire in southern Africa: A meta-analysis using long-term field data and satellite-derived burnt area data. *Glob. Ecol. Biogeogr.* **2010**, *19*, 794–809. [CrossRef]
323. Mbow, C.; Goita, K.; Bénié, G.B. Spectral indices and fire behavior simulation for fire risk assessment in savanna ecosystems. *Remote Sens. Environ.* **2004**, *91*, 1–13. [CrossRef]
324. Verhegghen, A.; Eva, H.; Ceccherini, G.; Achard, F.; Gond, V.; Gourlet-Fleury, S.; Cerutti, P.O. The Potential of Sentinel Satellites for Burnt Area Mapping and Monitoring in the Congo Basin Forests. *Remote Sens.* **2016**, *8*, 986. [CrossRef]
325. Philipp, M.B.; Levick, S.R. Exploring the Potential of C-Band SAR in Contributing to Burn Severity Mapping in Tropical Savanna. *Remote Sens.* **2020**, *12*, 49. [CrossRef]
326. Hudak, A.T.; Fairbanks, D.H.K.; Brockett, B.H. Trends in fire patterns in a southern African savanna under alternative land use practices. *Agric. Ecosyst. Environ.* **2004**, *101*, 307–325. [CrossRef]
327. Militino, A.F.; Ugarte, M.D.; Pérez-Goya, U. An Introduction to the Spatio-Temporal Analysis of Satellite Remote Sensing Data for Geostatisticians. In *Handbook of Mathematical Geosciences*; Daya Sagar, B.S., Cheng, Q., Agterberg, F., Eds.; Springer International Publishing: Cham, Switzerland, 2018; pp. 239–253. ISBN 978-3-319-78998-9.